IDO-17038
January 1965

RADIOLOGICAL ASPECTS OF SNAPTRAN 2/10A-3 DESTRUCTIVE TEST

O. L. Cordes, R. P. Bird,
G. A. Dinneen, and J. R. Fielding

PHILLIPS PETROLEUM COMPANY
ATOMIC ENERGY DIVISION

NATIONAL REACTOR TESTING STATION
US ATOMIC ENERGY COMMISSION

PRINTED IN USA. PRICE $3.00. AVAILABLE FROM THE CLEARINGHOUSE FOR FEDERAL SCIENTIFIC AND TECHNICAL INFORMATION, NATIONAL BUREAU OF STANDARDS, U. S. DEPARTMENT OF COMMERCE, SPRINGFIELD, VIRGINIA

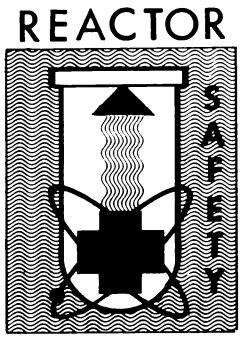

STEP PROJECT

IDO-17038
AEC Research and Development Report
Aerospace Safety
TID-4500 (36th Ed.)
Issued: January 1965

RADIOLOGICAL ASPECTS OF SNAPTRAN 2/10A-3 DESTRUCTIVE TEST

by

O. L. Cordes
R. P. Bird (AEC)
G. A. Dinneen
J. R. Fielding

PHILLIPS
PETROLEUM
COMPANY

Atomic Energy Division
Contract AT(10-1)-205
Idaho Operations Office
U. S. ATOMIC ENERGY COMMISSION

ACKNOWLEDGEMENTS

Valuable assistance in the preparation of this report was given by many members of the Phillips Health and Safety Branch, the STEP Staff, the USAEC-ID Health and Safety Branch, and the U. S. Weather Bureau. In particular, the authors wish to thank J. K. Sommers, R. S. Peterson, and A. L. Smith for their aid in the collection and reduction of data; W. E. Kessler and G. B. Matheney for valuable assistance and suggestions in the report content and form; J. K. Warkentin, who prepared the radiological calculation; R. D. Fletcher for fuel analysis data; E. H. Markee of the U. S. Weather Bureau for assistance in preparation of Appendix A; and the MTR Radiation Measurement Group, the ICPP Analytical Branch, and the USAEC-ID Analytical Chemistry Branch for analytical work.

ABSTRACT

Information for the Aerospace Safety Program was acquired by subjecting a SNAP 2/10A reactor to a simulated water immersion accident which resulted in destructive disassembly of the reactor core. This report describes in detail an extensive monitoring grid used to monitor the radiological effects of the destructive excursion and subsequent release of fission products. An analysis of the data is included which indicates that the direct radiation hazards were low and that the only fission products released to the environment were less than 4 percent of the noble fission gases. Halogens that escaped from the fuel were retained in the environmental water.

SUMMARY

A SNAP 2/10A reactor core was subjected to rapid water immersion such as might result from an aborted space mission in order to evaluate the radiological hazards of such an incident. This test was conducted as part of the Atomic Energy Commission's Nuclear Safety Program and was designated as the SNAPTRAN 2/10A-3 water immersion test.

The immersion test which resulted in destructive disassembly of the reactor core and vessel was conducted April 1, 1964, in Idaho at the National Reactor Testing Station by the Nuclear Safety Engineering and Test Branch of Phillips Petroleum Company.

Only slight airborne radiological effects resulted from the destructive test. More than 99 percent of the fission products were retained in the environmental water and reactor fuel remains. The halogens that escaped from the fuel were retained in the water, and, as a result, no airborne iodine was detected. The only fission products detected in the radioactive cloud were noble gases and their daughters. It is estimated that on the order of 3 percent of the noble fission gases generated during the destructive excursion was released. The radioactivity from the cloud decreased to background at about 21 miles downwind. Sensitive monitors revealed no airborne beryllium contamination in the cloud or in the near vicinity of the reactor.

Direct radiation likewise was moderate. The highest measured gamma dose was 150 rem at a point twelve feet directly above the reactor. This measurement encompassed the direct radiation from the burst and the fission product decay during a one-hour period following the burst. The radiation level at the rim of the environmental tank two hours after the test was less than 25 rem/hr. At 24 hours after the test, this had reduced to about 3 rem/hr. The peak dose rate from the cloud at 100 meters downwind was approximately 2 rem/hr.

As a result of this test, it can be concluded that no significant radiological hazard to the public will result from the rapid water immersion of a SNAP 2/10A reactor. In addition, the information gained from the test will assist in predicting the behavior of similarly fueled reactors under accident conditions.

RADIOLOGICAL ASPECTS OF
SNAPTRAN 2/10A-3 DESTRUCTIVE TEST

CONTENTS

ACKNOWLEDGEMENTS ii

ABSTRACT iii

SUMMARY iv

I. INTRODUCTION 1

1. DESCRIPTION OF REACTOR 1

2. RADIOLOGICAL MONITORING PROGRAM 3

3. MONITORING NETWORK 5

II. INSTRUMENTATION AND EQUIPMENT 9

1. AIR SAMPLERS AND FILTERS 9

1.1 High-Volume Air Sampler 9
1.2 Noble-Fission-Gas Detector 10
1.3 Particle Size Samplers 10
1.4 Filters 12

2. DEPOSITION SAMPLERS 12

2.1 Fallout Plates 12
2.2 Water Samplers 12

3. DOSIMETERS 13

3.1 Film Packet Dosimeters 13
3.2 Subsurface "Well" Dosimeters 13
3.3 High Range Dosimeters 13
3.4 Neutron Dosimeters 14
3.5 Phantoms 14
3.6 Remote Radiation Monitors 14
3.7 Prompt Gamma Radiation Dose Measurements 15

4. METEROLOGICAL INSTRUMENTS 15

4.1 Wind Field Measurements 15
4.2 Diffusion Parameter Measurements 15
4.3 Cloud Trajectory Measurements 15

5. AUXILIARY EQUIPMENT 17

5.1 Radiological Tower and Stack Cloud-Height Samplers 17

5.2 "Clothesline" Device 17
5.3 Air Support 17
5.4 Telemetering Network 17

III. TEST OPERATION 19

IV. PRESENTATION OF DATA 21

1. FISSION-PRODUCT DISTRIBUTION 21

1.1 Radioactive Cloud 21
1.2 Fission Products In Water 24
1.3 Fuel Analysis 25

2. DIRECT RADIATION MEASUREMENTS 28

2.1 Excursion Prompt Radiation 28
2.2 Fission-Product Delayed Radiation 29
2.3 Cloud Radiation 29
2.4 Film Dosimeters on the Grid 29
2.5 Film Dosimeters on the Radiological Tower 33
2.6 Dosimeters Other Than Film Dosimeters 33
2.7 Phantom Doses 33

3. BERYLLIUM RELEASE 34

4. METEOROLOGICAL PARAMETERS 34

V. DATA ANALYSIS 39

1. IODINE DISTRIBUTION 39

1.1 Available Iodine 39
1.2 Iodine Released to the Cloud 39
1.3 Iodine Released to the Water 40
1.4 Iodine Retained in the Fuel 40
1.5 Iodine Plate-Out 40
1.6 Iodine Balance Summary 41

2. FRACTION OF NOBLE GAS RELEASE 41

2.1 Diffusion Calculations Using Kr-91, Kr-92, and Xe-139 Decay Chains 41
2.2 Cloud Volume Calculation -- Xe-138 Decay Chain 42
2.3 Fuel Analysis Xe-137 Chain 42
2.4 Kr-85 Fuel Analysis 43
2.5 Summary of Noble Fission-Gas Release 43

3. DIRECT RADIATION ANALYSES 43

3.1 Comparison of Doses 43

4. MAXIMUM DIRECT RADIATION HAZARD 46

VII. CONCLUSIONS 48

APPENDIX A -- ESTIMATES OF ATMOSPHERIC DIFFUSION AND NOBLE FISSION-GAS RELEASE 51

1. RADIOACTIVE DECAY 53

2. SAMPLING RATES 53

3. FILTER EFFICIENCY 53

4. UNSAMPLED PORTION OF PARENT GAS 53

II. REFERENCES 60

APPENDIX B -- DIFFUSION CALCULATION TECHNIQUES 61

I. ANALYTICAL TECHNIQUES -- EQUATIONS USED 63

1. DIRECT RADIATION FROM POWER BURST 63

2. DIRECT RADIATION FROM FISSION-PRODUCT DECAY 64

2.1 Disc Source 64
2.2 Line Source 65
2.3 Cylindrical Source 65

II. ASSUMPTIONS 67

III. REFERENCES 68

FIGURES

1. SNAPTRAN 2/10A-3 core cross section 2

2. SNAPTRAN 2/10A-3 reactor and flatcar assembly 3

3. SNAPTRAN 2/10A-3 reactor with binal sleeve 4

4. Radiological monitoring grid beyond a radius of 1600 meters 5

5. Radiological monitoring grid to a radius of 100 meters 6

6. Radiological monitoring grid to a radius of 300 meters 7

7. Radiological monitoring grid to a radius of 2500 meters 7

8. Typical grid station, consisting of a fallout plate, a film dosimeter, a high-volume air sampler, and a fission-gas detector 8

9. High-volume air sampler 9

10. Modified high-volume air sampler 10
11. Fission-gas detector 11
12. Flow diagram of fission-gas detector 11
13. Phantoms approximating man's torso in size and composition 14
14. Remote telemetering station 17
15. Layout and cross section of the IET test area 20
16. SNAPTRAN 2/10A-3 core layout 26
17. Fuel-rod remains, arranged according to core layout 27
18. Prompt gamma dose rate from excursion 29
19. Dose measurements on and around environmental tank 31
20. Cloud dose rate measurements at downwind locations 32
21. Grid radiological dose measurements 34
22. Dose measurements from radiological tower locations 35
23. Phantom film-dosimeter results 37
24. Isopleths of values of μcurie-sec/m^3 for Sr-91 41
25. Gamma dose data from radiological tower locations -- measured versus calculated 45
26. Gamma dose data from locations at inner edge of environmental tank -- measured versus calculated 46
27. Total integrated dose from direct radiation with no shielding considered 47
A-1. Instantaneous release model 55
A-2. High volume activity measured at 2.28 hours after test 56
A-3. Predicted and measured isotope ratios 56
A-4. Lateral cloud spread, σ_y, with distance downwind 57
A-5. Peak time -- integrated concentrations at each sampling distance downwind 58

TABLES

I. Cloud Size Versus Distance 21

II. Air Sampler Filter Data 22

III. Water Analysis Data 24

IV. Fuel Analysis Data 25

V. Fuel Particle Size Range 28

VI. Neutron Measurements 30

VII. Radiological Measurements Inside Test Cell Area 32

VIII. Grid Film-Dosimeter Data 33

IX. High Range Dosimeter Data 36

X. Meteorological Parameters 37

XI. Turbulence and Diffusion Parameters 38

XII. Curie Code Data for Iodine 39

XIII. Calculated Versus Measured Radiation Doses 44

I. INTRODUCTION

As part of the space effort of the United States, a number of small nuclear reactors are under development to supply auxiliary power for space vehicles. These SNAP (Systems for Nuclear Auxiliary Power) reactors, which cannot be provided with the usual engineering safeguards, such as biological shielding because of weight limitations, pose unique nuclear safety problems. The Atomic Energy Commission, therefore, has established, as part of its overall nuclear safety effort, a test program to determine the radiological consequences of potential nuclear incidents involving these reactors under actual accident conditions and to provide information on the kinetic behavior of the reactor systems. This program, which is being conducted for the Atomic Energy Commission by Phillips Petroleum Company at the National Reactor Testing Station (NRTS), has been designated the SNAPTRAN program, with the first reactor tested being the SNAP 2/10A.

One conceivable mechanism for the initiation of a nuclear incident is the immersion of the reactor in water. Such an event could occur during transport, as an aftermath of an explosion on the launch pad, or during a launch abort over water. The resulting super-critical configuration would result in a power excursion accompanied by the release of radioactive fission products into the water and the surrounding environment.

At 1144 hours on April 1, 1964, the Engineering Test Branch (ETB) of Phillips Petroleum Company initiated a destructive excursion with a SNAP 2/10A reactor to simulate the water immersion type of accident. This test was designated as the SNAPTRAN 2/10A-3 Water Immersion Destructive Test.

The purpose of this report is to present the radiological data obtained from the destructive test. The data have been evaluated for several parameters of interest to aid in the extension of the experience gained from this test to safety evaluation of reactors in general and the SNAP reactors in particular. The three general areas examined in this report are: (a) distribution of radioactive iodine, (b) fraction and type of fission products released, and (c) direct radiation doses and dose rates. A description of the radiological monitoring network used to obtain the radiological data is also included along with a brief description of each type of instrument used.

The kinetic behavior of the reactor during the SNAPTRAN 2/10A-3 test has been reported in a separate report, IDO-17019 [1].

1. DESCRIPTION OF REACTOR

The SNAPTRAN 2/10A-3 reactor was a modified SNAP 2/10A Flight-System reactor. The core was a cylinder approximately 9 inches in diameter by 13 inches long. The fuel rods consisted of an alloy of zirconium-hydride and 10 weight percent of fully enriched uranium, clad with Hastelloy-N. The core, as shown in the cross section view in Figure 1, was composed of six beryllium inserts and thirty-seven fuel rods, arranged in a close-packed hexagonal array containing 4.75 kg of U-235 and 464 g-moles of hydrogen. The core was contained in a stainless steel vessel having a wall thickness of

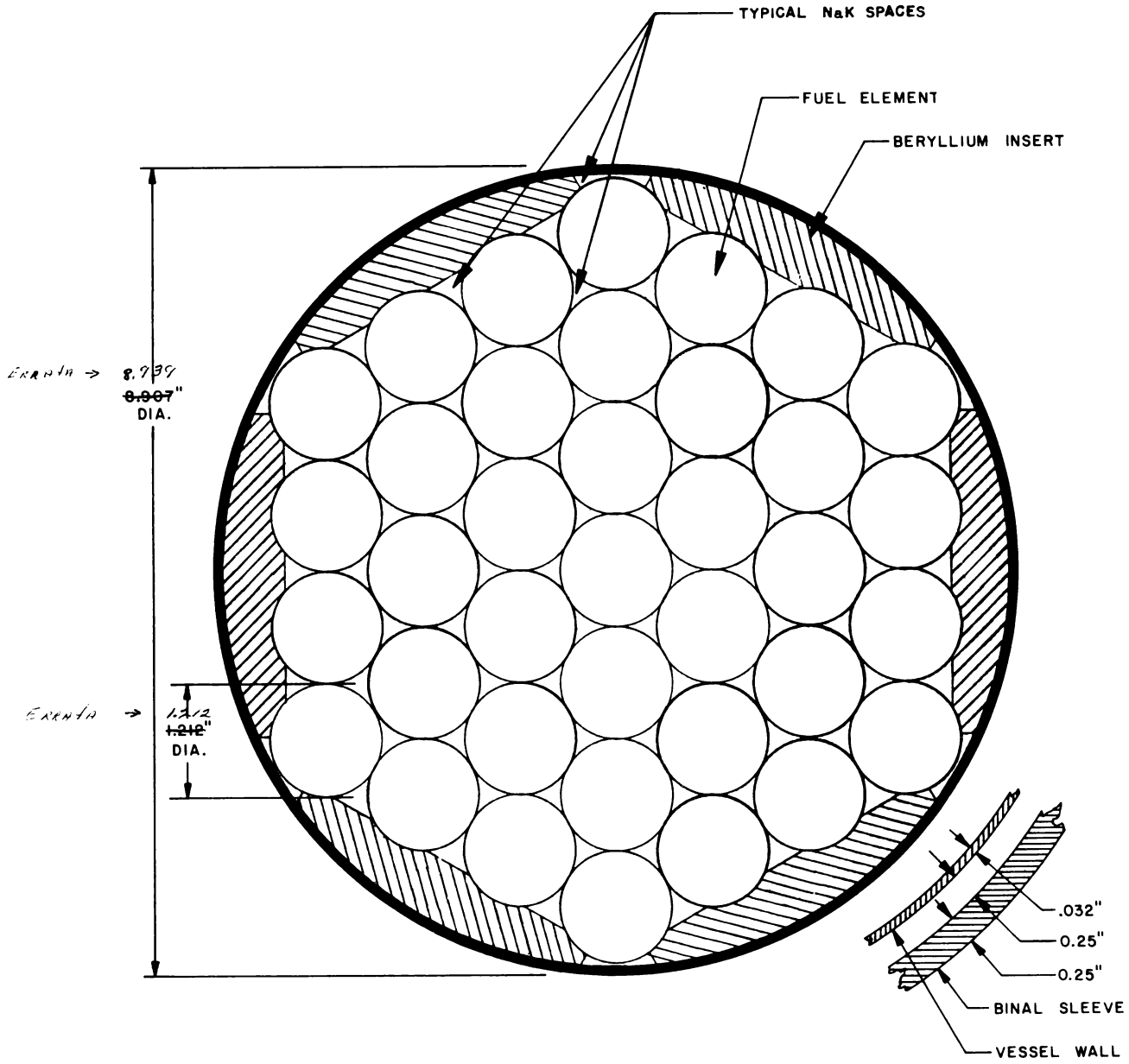

Fig. 1 SNAPTRAN 2/10A-3 core cross section.

0.032 inch. The reactor vessel was modified from the "flight-system" vessel to allow access for in-core instrumentation and to contain the NaK reactor coolant. Approximately seven pounds of NaK coolant were contained in the interstitial spaces in and around the fuel.

The reactor, as shown in Figure 2, was housed in an environmental tank with an internal diameter of 14 feet and a height of 10 feet. The size of the tank was selected to simulate a large body of water and still remain small enough to facilitate pressure measurements and evaluation of other phenomena, such as metal-water reactions and secondary criticalities. The environmental tank and associated equipment were mounted on a four-rail, railroad-type dolly for ease in transportation between the "Hot Shop" examination area and the test pad (Initial Engineering Test Facility, IET).

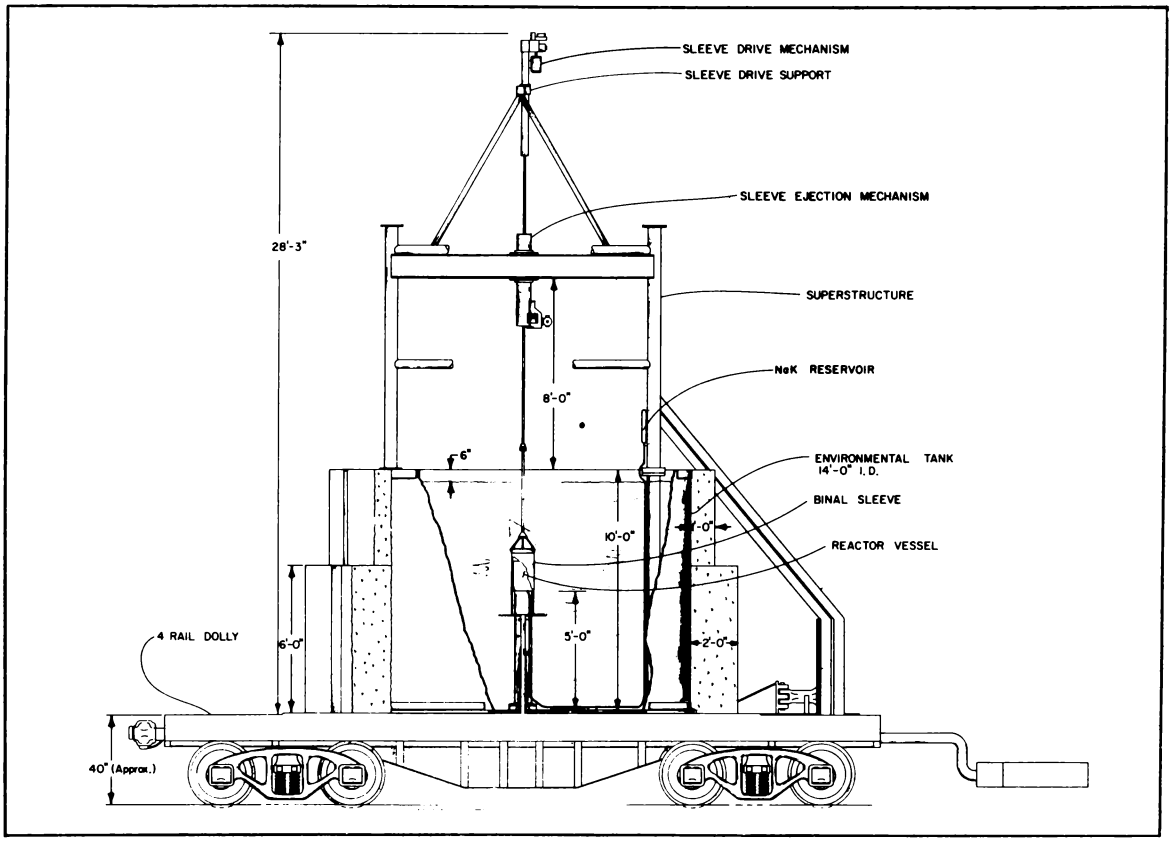

Fig. 2 SNAPTRAN 2/10A-3 reactor and flatcar assembly.

The reactor was controlled by the axial position of a 1/4-inch-thick neutron-absorbing binal sleeve which surrounded the reactor (Figure 3). Initiation of the destructive excursion was accomplished by a pyrotechnic actuator which was connected to the binal sleeve. The pyrotechnic actuator, powered by a black powder charge, removed the control sleeve from the reactor at velocities comparable to those at which the reactor would enter the water from a launch abort. Under these conditions, the destructive test approached the maximum credible accident for a water immersion incident.

2. RADIOLOGICAL MONITORING PROGRAM

An extensive monitoring program was undertaken to measure and evaluate the radiological consequences of the SNAPTRAN 2/10A-3 destructive test. The primary purpose of the program was the detailed evaluation of the test consequences; however, monitoring was also provided for quick assessment of test hazards in order to assure that no off-site hazard to the public occurred. Some additional radiological and meteorological measurements were made for research, aside from the test objective of evaluating the SNAP accident consequences. The monitoring program was the joint effort of the Engineering Test Branch and the Health and Safety Branch of Phillips Petroleum Company (PPCo. H and S), the Health and Safety Division of the AEC Idaho Operations Office (ID H and S), and the U. S. Weather Bureau Research Station located at the NRTS.

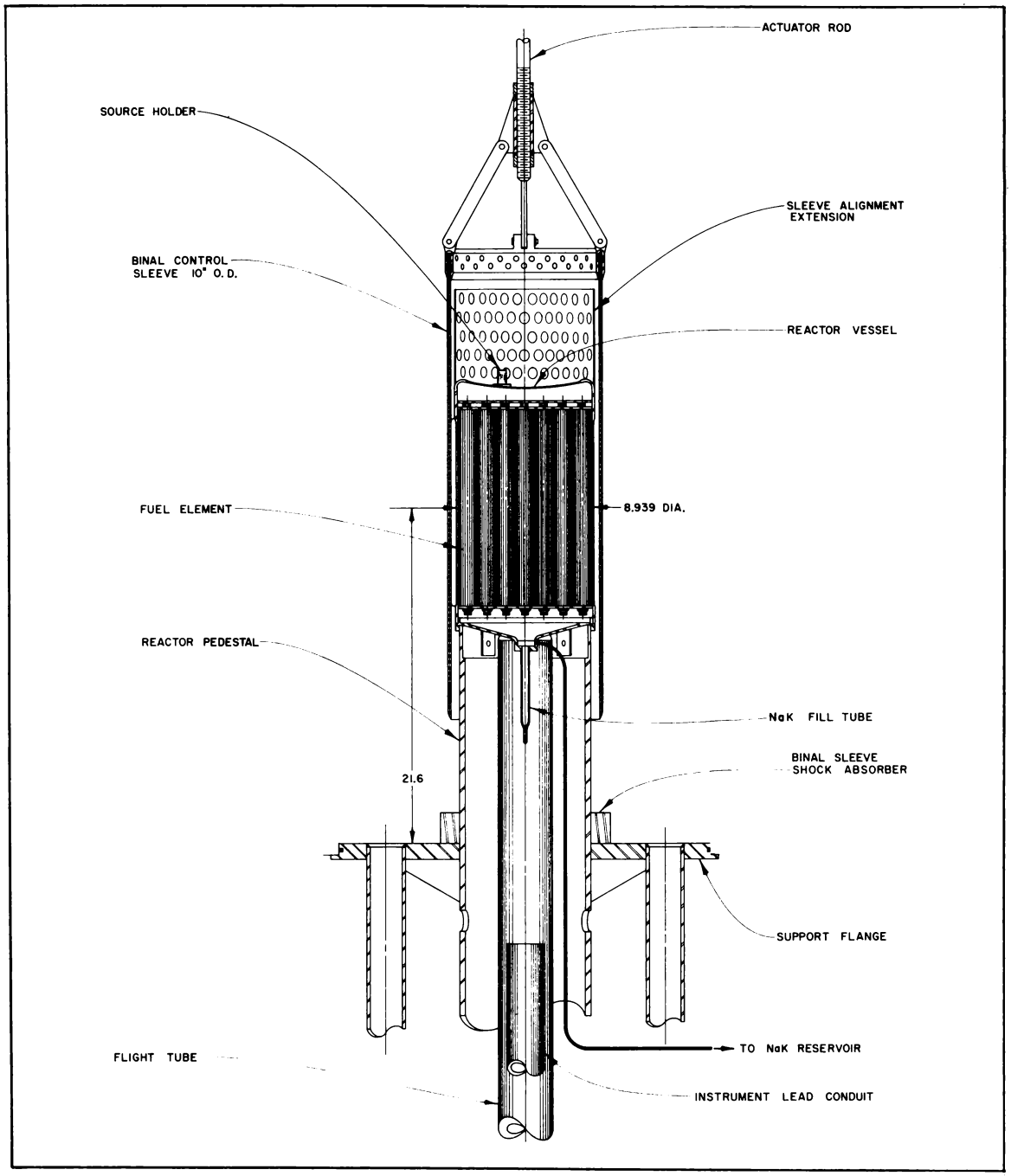

Fig. 3 SNAPTRAN 2/10A-3 reactor with binal sleeve.

The division of responsibility for the monitoring was as follows: Phillips Petroleum Company Health and Safety Branch was responsible for the radiological monitoring out to a concentric arc approximately 1600 meters from the reactor; ID Health and Safety was responsible for the radiological monitoring extending beyond 1600 meters, plus the random instrumentation that was placed in the surrounding towns and other off-site locations (Figure 4). The U. S. Weather Bureau was responsible for measuring the meteorological conditions (wind velocity, direction, and short term fluctuations) over the entire monitoring grid and for determining the atmospheric diffusion conditions existing during the test.

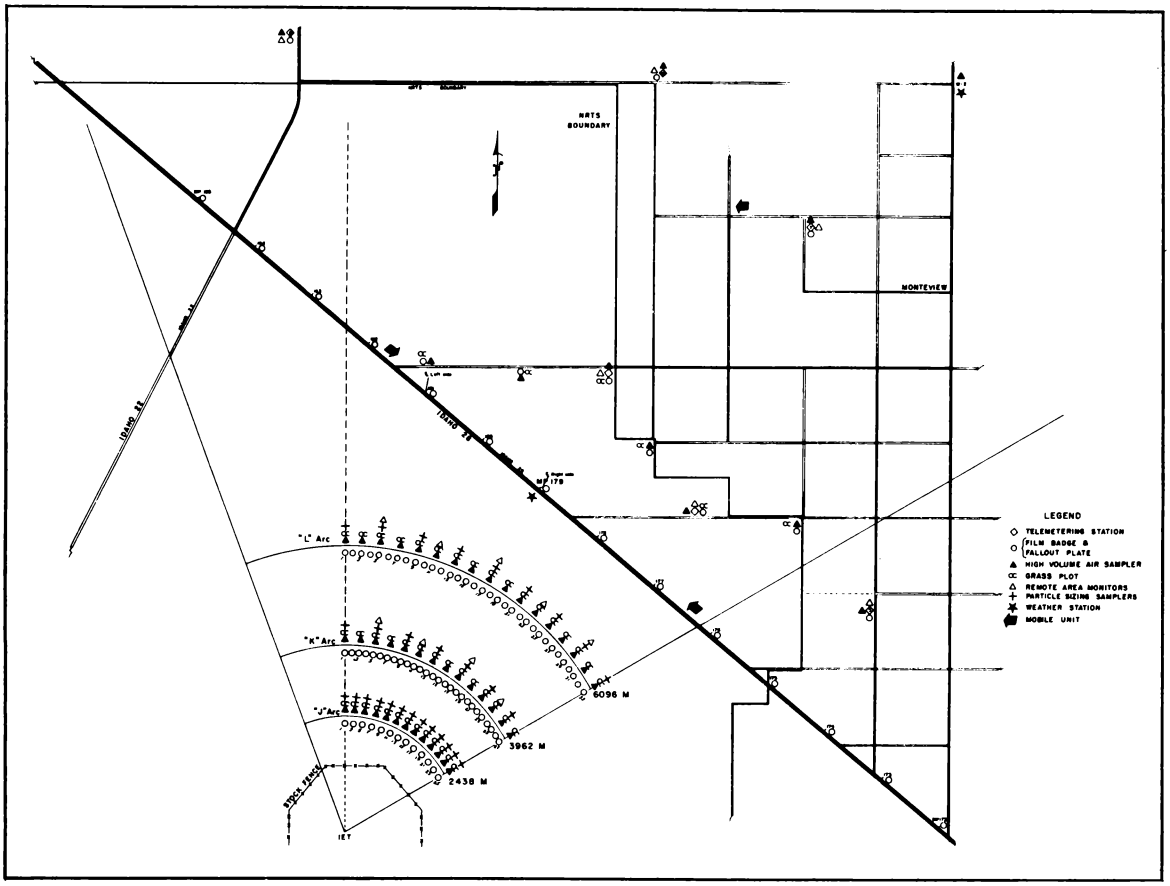

Fig. 4 Radiological monitoring grid beyond a radius of 1600 meters.

3. MONITORING NETWORK

A radiological monitoring network was set up to measure the radiological consequences of the destructive test (including measurements of fission product release, direct gamma and neutron doses, spread of airborne contamination, and the release of beryllium). The monitoring network included a radiological monitoring grid (Figures 4, 5, 6, and 7), which was set up as a series of concentric arcs with the reactor test pad at the center. A heavy concentration of sampling equipment was placed in a 60° sector, oriented with the centerline of the proposed "cloud" trajectory 30° east of true north. The types of samplers used and the placement of the instrumentation of the monitoring grid are shown in Figures 4, 5, 6, and 7, with a typical grid station shown in Figure 8. In addition to the grid instrumentation, samplers were located in various areas near the off-site populated regions, in the surrounding towns, and on the test pad immediately surrounding the reactor.

Weather played an important role in the destructive test as a specific set of weather conditions had to be met before the test could be initiated. The potential hazards of the test, particularly the release of fission products and beryllium to the atmosphere, required that the test be prohibited until acceptable

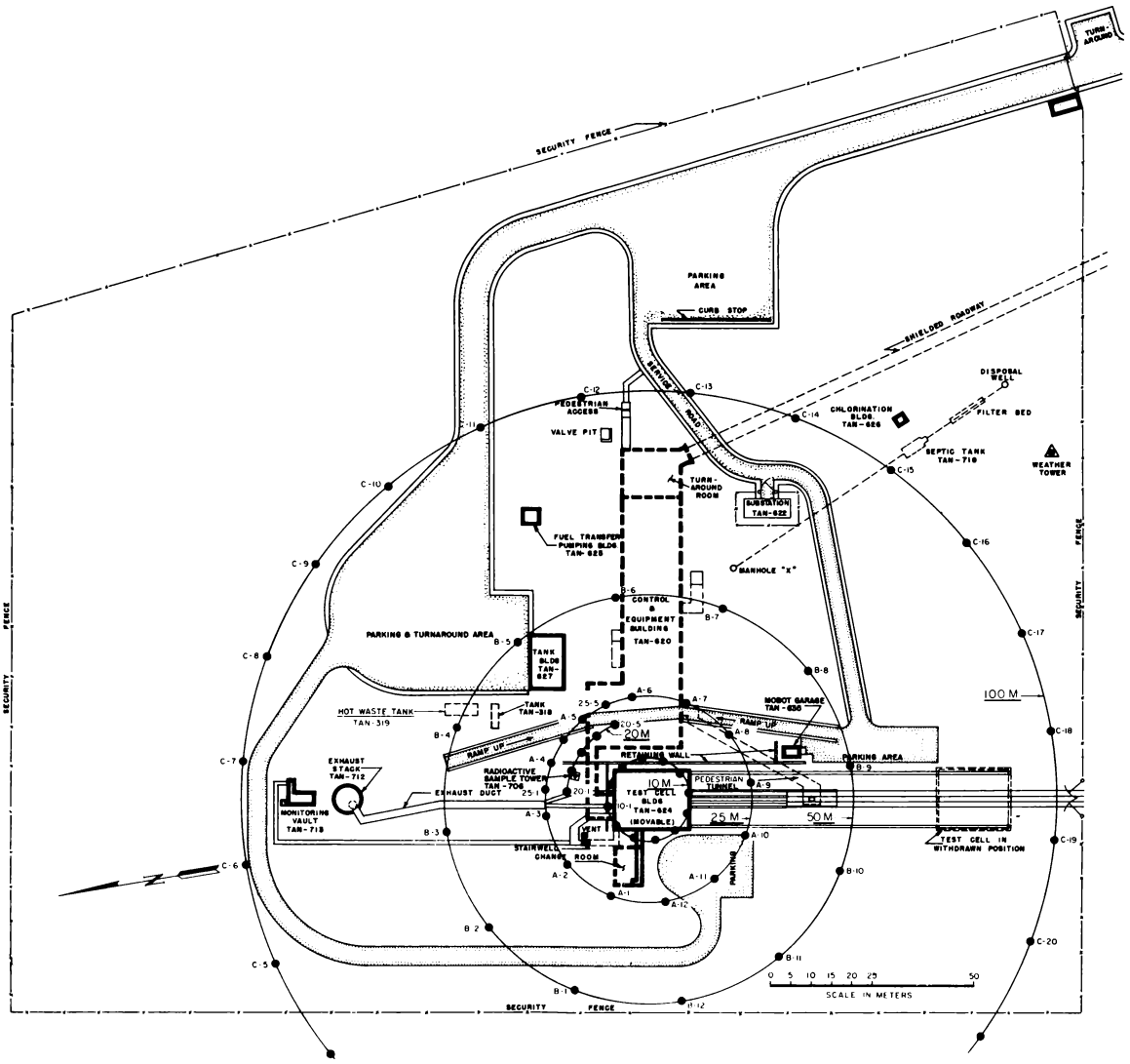

Fig. 5 Radiological monitoring grid to a radius of 100 meters.

meteorological conditions prevailed. These conditions, established by the Idaho Operations Office of the AEC in conjunction with the U. S. Weather Bureau, were:

(1) Lapse (unstable) conditions, to persist a minimum of three hours after the test to ensure adequate diffusion conditions

(2) Mean wind direction in the sector between 180 and 240°, with the allowance of an additional 20° on each side of the sector for short term wind fluctuations

(3) Wind speed between 10 and 30 miles per hour, the lower limit to ensure reliability for forecasting a persistent wind direction and the upper limit to assure safe aerial monitoring

(4) No precipitation in the area, in order to maintain good sampling conditions and to prevent localized washout of radioactive material.

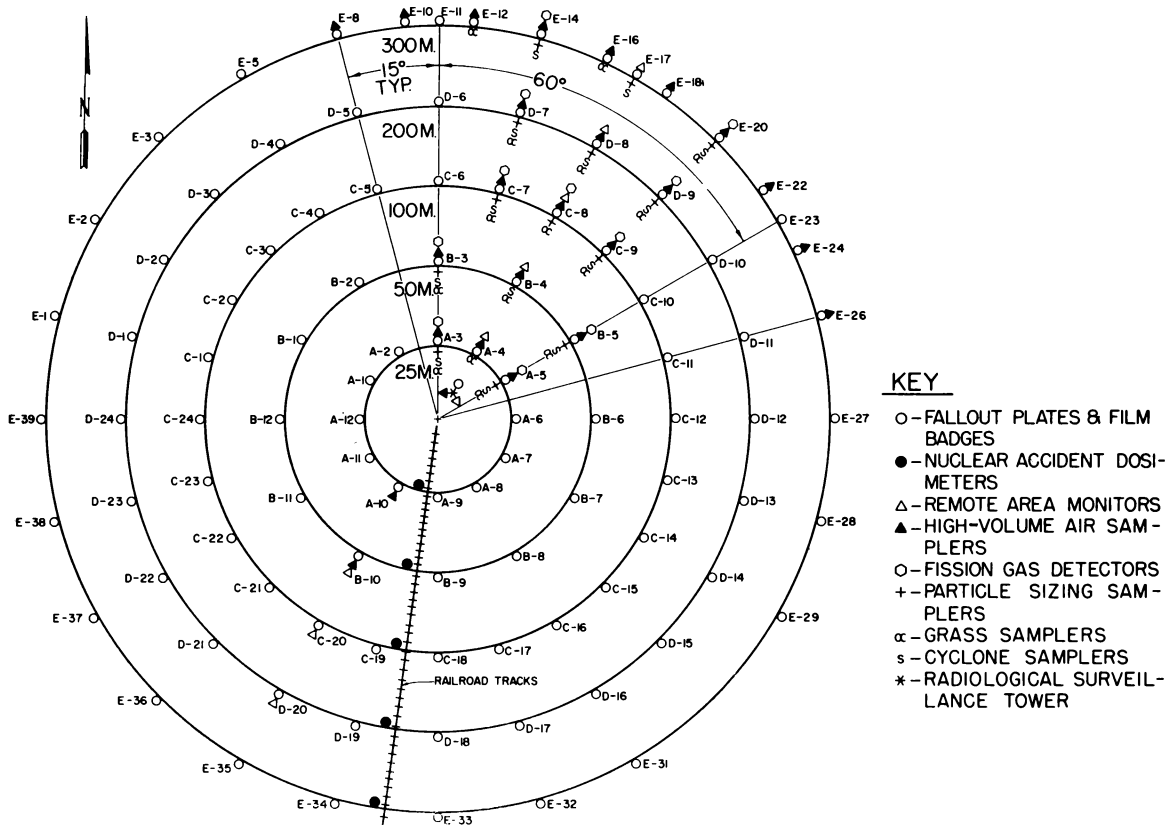

Fig. 6 Radiological monitoring grid to a radius of 300 meters.

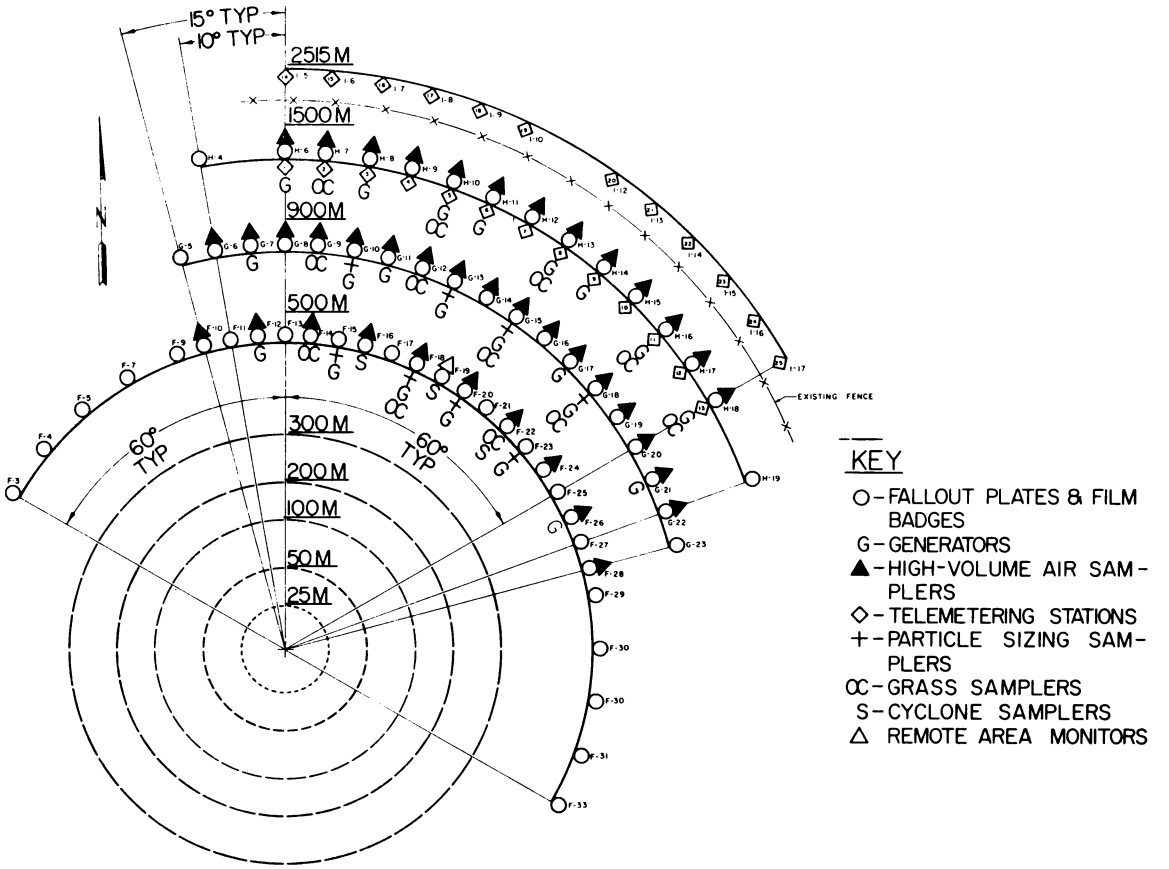

Fig. 7 Radiological monitoring grid to a radius of 2500 meters.

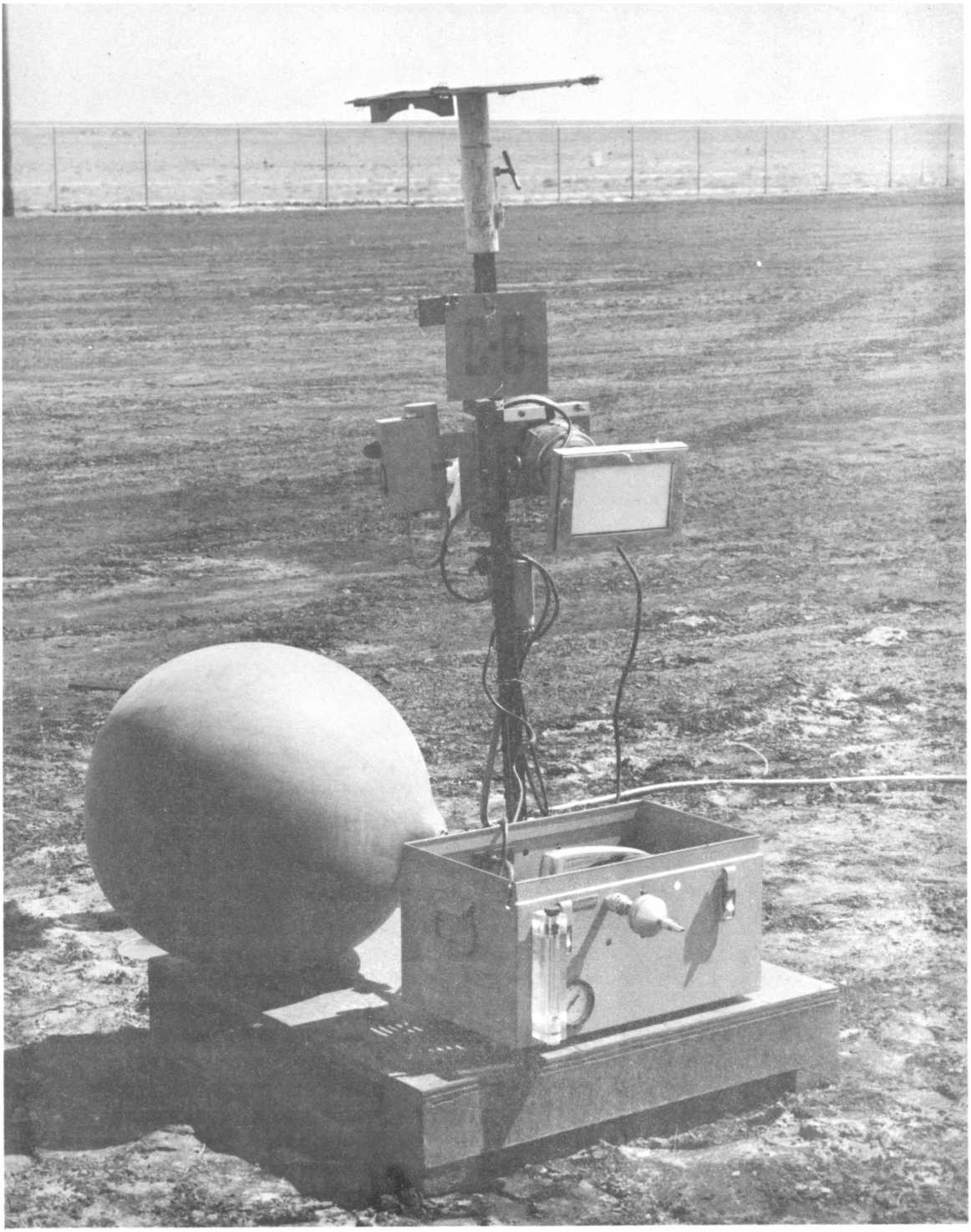

Fig. 8 Typical grid station, consisting of a fallout plate, a film dosimeter, a high-volume air sampler, and a fission-gas detector.

II. INSTRUMENTATION AND EQUIPMENT

A wide variety of instrumentation was required to measure the radiological consequences of the destructive test. Details, descriptions, and the purposes of the instrumentation and auxiliary equipment used are given in the following section.

1. AIR SAMPLERS AND FILTERS

1.1 High-Volume Air Sampler

The staplex model, high-volume air sampler, Figure 9, was selected for use during the destructive test monitoring. This sampler was modified to draw

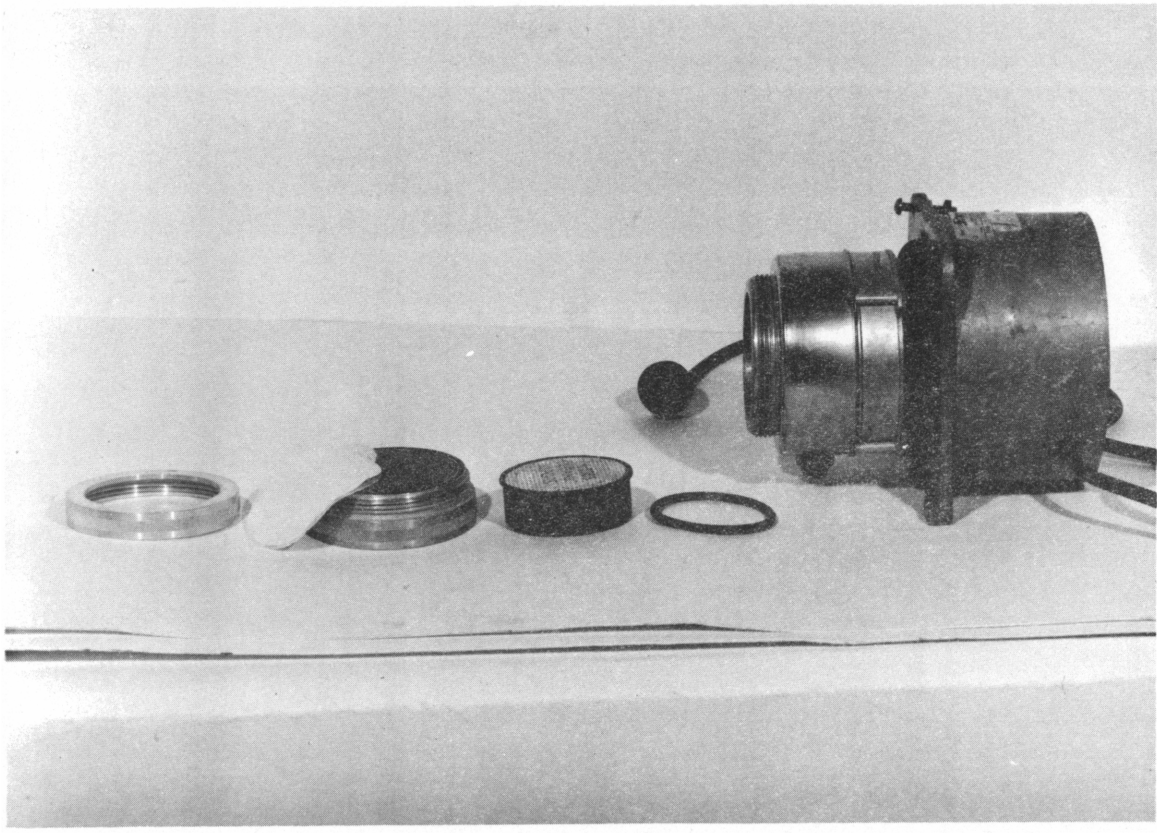

Fig. 9 High-volume air sampler.

a large volume of air through a four-inch-diameter particulate filter, backed by a standard one-inch-deep charcoal cartridge for collecting iodine. With this arrangement, the average flowrate through these samplers was approximately 22 cfm. Some of these samplers (Figure 10) were modified to obtain greater flowrates (approximately 40 cfm) by enlarging the inlet side of the sampler and

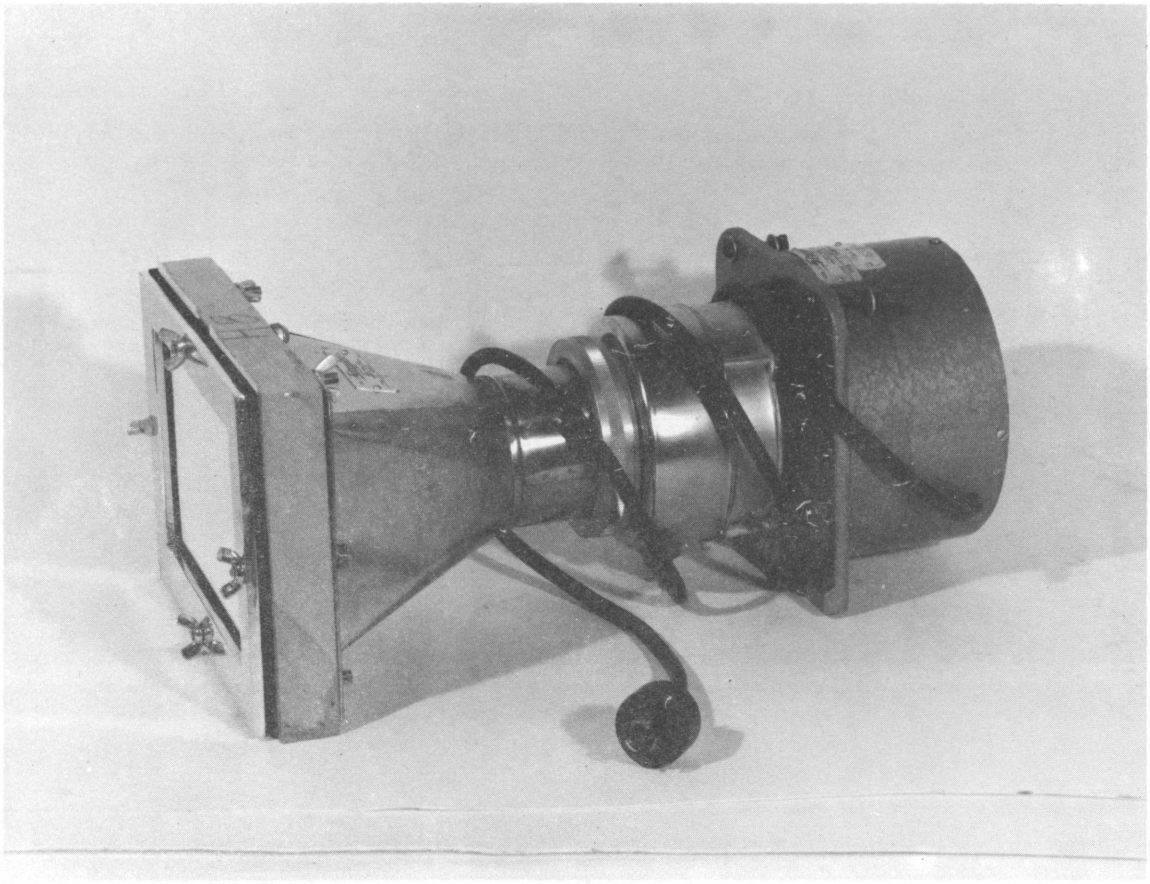

Fig. 10 Modified high-volume air sampler.

allowing the air to be drawn through two four-inch-diameter filters, each backed by a charcoal cartridge.

1.2 Noble-Fission-Gas Detector

The fission-gas detectors were designed to sample the radioactive noble gas concentration in the cloud near ground level. The gas concentration is measured by drawing a sample of the cloud through a high-efficiency filter into an airtight balloon, Figures 11 and 12. The air was pulled into the balloon while the cloud was passing, and the noble gases were allowed to decay to their particulate daughters for a prescribed length of time, after which the ballon was deflated through a second high-efficiency filter. The amount of daughter product activity trapped on the second filter and plated out in the balloon was measured by gamma-ray counting. This information, using the known half-lives and decay chains, makes it possible to calculate the amount of noble gases trapped in the balloon.

1.3 Particle Size Samplers

The three types of particle-sizing samplers used on the grid were: cyclone sampler [2], the Unico cascade impactor [3], and the Andersen sampler [4].

The cyclone sampler is a two-stage collector consisting of a cyclone sampling device in series with a high-efficiency filter. The cyclone stage

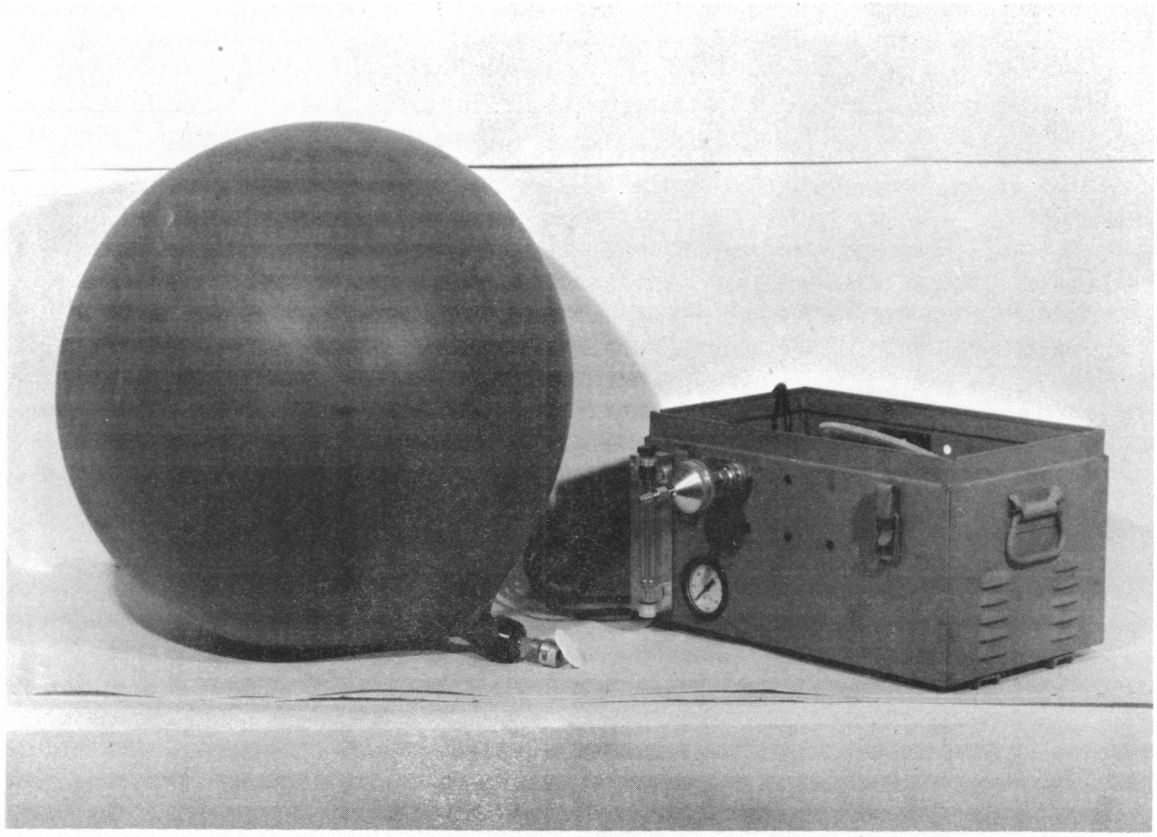

Fig. 11 Fission-gas detector.

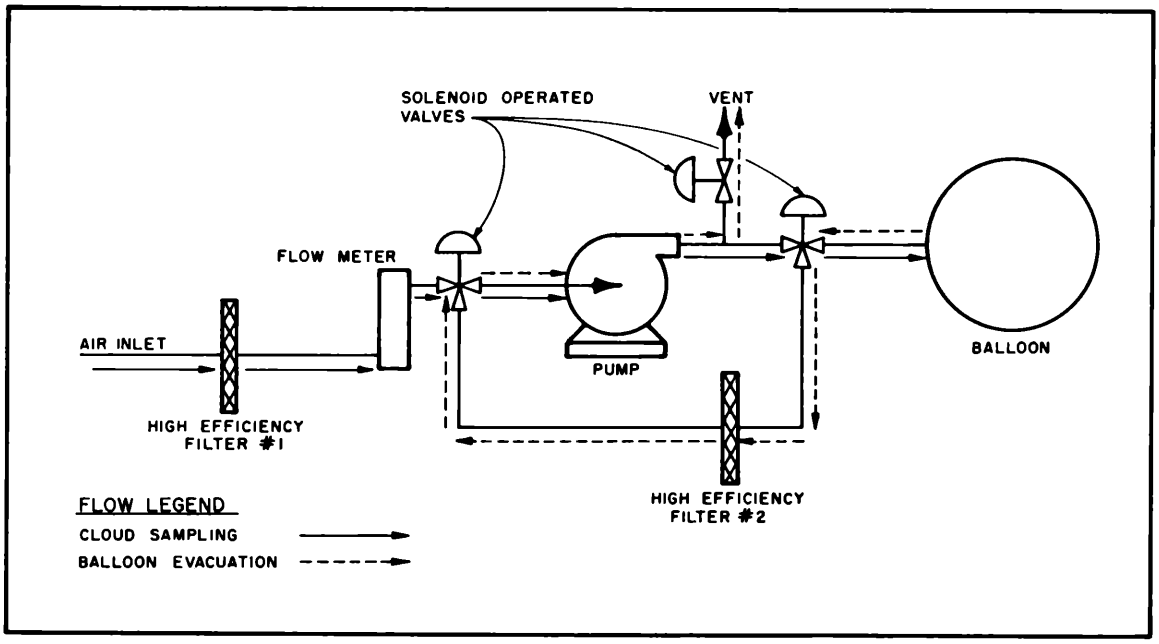

Fig. 12 Flow diagram of fission-gas detector.

captures the larger particles, ie, those above 10 microns in diameter. The smaller particles (less than 10 microns) are captured by the backup filter.

The Unico sampler is a cascade-type impactor with four deposition stages and a backup filter. Mass median sizes, from 20 microns to 0.5 micron in diameter, can be measured.

The Andersen sampler consists of six stages, in series, through which the sample of air is drawn. Each stage contains a sizing plate, perforated with 400 holes, and a backup, stainless steel plate, coated with a silicone particle adhesive. The size of the holes is constant for each stage but is smaller for each succeeding stage. Consequently, the jet velocity increases in each succeeding stage. At a sampling rate of 1 cfm, the sampler is designed so that any airborne particles of 1 micron or larger will be distributed among the stages according to their size. The remaining particles are collected on a backup filter.

1.4 Filters

High-efficiency filtering media, consisting of commercially available spun polystyrene pads [5], were used on all particulate air samplers during the test. This material has the advantage of low flow resistance while maintaining a high collection efficiency (greater than 99 percent for particles greater than 0.1 μ). In addition, the filters made from this media contained no beryllium, which made them useful for beryllium monitoring.

2. DEPOSITION SAMPLERS

2.1 Fallout Plates

Fallout plates, made from a sticky-type paper, were used for obtaining the fallout distribution, concentration, and isotopic identification of the fission products deposited on the grid from the radioactive cloud. Two sizes of fallout plates were used, 12 by 15 inches and 4 by 9 inches. The larger plates were used close to the reactor in the 60° downwind grid sector to assure that a highly sensitive measurement was obtained. The smaller plates were used on the distant arcs where the number of samplers made the economics of using the smaller size attractive.

2.2 Water Samplers

To obtain a measure of the instantaneous release of fission products from the fuel into the water, samplers were set up around the reactor to catch the water ejected during the excursion. These open-top samplers consisted of a series of water catch cans and long compartmented trays. In addition, sample bombs were designed to draw water samples from the water that remained in the environmental tank following the test.

3. DOSIMETERS

3.1 Film Packet Dosimeters

Two types of film dosimeters were used in the test to measure beta and gamma exposures. Both types contained Dupont film packets with sensitive and insensitive film for measuring high and low range exposure. One type [6] had the film packet hermetically sealed in special red plastic designed to reduce the effect of exposure to sunlight. This type was used where they could be positioned in order to reduce the time required to prepare the grid for the test. The other type of dosimeter contained the film packets in a plastic film-badge holder like the personnel film-badge dosimeter worn by nearly all NRTS personnel [7]. This second type of holder provided windows and shields over the film packet, making it possible to discriminate between beta and gamma radiation exposures. The minimum detectable dose of these film dosimeters is 10 mrem.

3.2 Subsurface "Well" Dosimeters

To measure the cloud radiation, a small "well" was dug at each grid station on the 60° sector out to, and including, the "E" arc. These "wells", approximately four inches deep, were fitted with a metal can. Film badge dosimeters were placed in these cans where they would be shielded from the direct radiation from the reactor and fallout. In this shielded position, the "well" dosimeters monitored only the radioactive cloud to give an integrated exposure reading for the radiation received from airborne radiation.

3.3 High Range Dosimeters

Since the possibility of high gamma doses from the reactor transient could not be ruled out, several types of high range dosimeters were installed in the immediate vicinity of the test cell.

Commercially available dosimeters with the following characteristics were purchased.

Dosimeter	Dose Range	Description
Chemical (tetrachloroethylene) EGG [a], Santa Barbara, Calif.	25 to 10^5 rem	5 ampoule packets, housed in 3-1/4 x 4-1/8 inch lithium can
Silver Phosphate Glass EGG, [a] Santa Barbara, Calif.	25 to 10^4 rem	5 glass rods, contained in 1/2-inch diameter x 1/2 inch high discriminatory shield
Cobalt Glass EGG [a], Santa Barbara, Calif.	10^4 to 2 x 10^6 rem	3 cobalt glass wafers, contained in a 1/2 x 3/4 inch high, energy discriminatory shield
Thermoluminescent Controls for Radiation Inc., Cambridge, Mass.	0.01 to 10^5 rem	Lithium fluoride phosphor, sealed in a 1/2 x 3/4 inch high, energy discriminatory shield

[a] Edgerton, Germeshausen, and Grier Inc.

3.4 Neutron Dosimeters

Several neutron-activation systems were used to measure the neutron spectrum and the neutron dose due to the reactor excursion. Six nuclear accident dosimeters (NADs) of the ORNL Hurst type [8] were placed around the reactor where they could be recovered as soon as possible after the test. Additional neutron activation samplers consisted of the NRTS personnel film dosimeter packet, samples of human hair, activation foil boxes, copper wire, and samples of blood.

The film-badge dosimeters contain the NRTS-ID personnel neutron-threshold detector incorporating sulfur, indium, gold foil, and cadmium-encased gold foil. These detectors measure neutron fluxes in the thermal and fast energy ranges. The sample of human hair was used to study the application of neutron activation of sulfur in hair as a measure of accidental neutron exposures. Similarly, the blood samples were analyzed for activation of sodium in blood as a measure of accidental neutron exposures. The copper wire and the activation foil boxes were used to evaluate materials that might improve nuclear accident monitoring techniques.

3.5 Phantoms

Film dosimeters were placed on phantoms (Figure 13) located near the reactor. These phantoms were large polyethylene bottles that approximated a man's torso in size and composition. They were filled with a solution which was tissue-equivalent so that gamma radiation attenuation and backscatter from man were simulated. Fifteen film dosimeters were placed at each phantom station: twelve on a belt surrounding the phantom, two hanging in free air below the phantom, and one centered inside the phantom. The phantom dosimeters provided not only a measure of radiation doses (both gamma and neutron) at the phantom stations but also a determination of the effect that personnel film-badge orientation may have on accident dose measurements [9].

Fig. 13 Phantoms approximating man's torso in size and compositon.

3.6 Remote Radiation Monitors

Twenty-one direct radiation monitors, commonly known as remote area monitors (RAMs) were used for the test. These remote units consisted of detector units, housed in weather-proof containers, which were connected by cable to recording and control panels. These monitors provided a measurement of the gamma dose rate from the cloud as a function of time and, thereby, gave a measurement of the radioactive cloud passage time.

3.7 Prompt Gamma Radiation Dose Measurements

Two sources of gamma radiation occur during a reactor excursion, that which accompanies the excursion (prompt) and that which occurs as a result of fission-product decay. Two types of instruments were used to determine the portion of the total dose that was contributed by the prompt radiation. The first of these consisted of film-badge stations with two identical film-badge dosimeters, one permanently attached to the station and the second held in place by an energized solenoid which released the badge following the power burst. The released badge dropped into a shielded receptacle buried in the ground, thereby measuring only the prompt radiation dose, while the duplicate badge measured the total integrated dose.

The second group of instruments were gamma-sensitive ion chambers located at various distances from the reactor. The primary purpose of these instruments was to measure the power history of the excursion; however by using the appropriate calibration constant, the output from these chambers was converted to gamma radiation dose measurements. The signals from these detectors were recorded on high-speed magnetic tape recorders, and this analog data was in turn processed by a computor system. With this arrangement, the detector and recording system was able to follow and trace the prompt gamma dose from the excursion as a function of time.

4. METEOROLOGICAL INSTRUMENTS

4.1 Wind Field Measurements

The wind field over the monitoring grid and downwind of the NRTS boundary was determined by using data from the wind speed and direction measuring instruments (aerovanes) at the 6.1- and 46-meter levels on the IET weather tower and by data from two remote radio-telemetering stations which measured wind speed and direction. These remote stations were both located beyond the NRTS boundaries, one at Monteview and the other along Idaho Highway 28.

4.2 Diffusion Parameter Measurements

Highly sensitive wind speed and direction instruments, cup anemometers and bivanes, at the 6.1- and 61-meter levels of the IET weather tower were used to measure the wind speed fluctuations and the vertical and horizontal wind direction fluctuations.

A weather balloon with a temperature-transmitting device was used to obtain a detailed vertical temperature profile to heights greater than the 61-meter IET weather tower.

4.3 Cloud Trajectory Measurements

A plastic tetrahedron balloon (tetroon) [10], designed to float at a constant air density level, was used to approximate the trajectory of the radioactive cloud from the test. The tetroon, carrying a small device called a transponder, was tracked along its trajectory by a Weather Bureau M-33 radar unit. The

transponder, when triggered by the radar, sends out its own strong signal which can be detected by the radar station at distances up to 50 miles.

5. AUXILIARY EQUIPMENT

5.1 Radiological Tower and Stack Cloud-Height Samplers

In order to measure the height of the radioactive cloud as it left the reactor area, sampling equipment was placed at various heights downwind of the reactor. Part of the elevated samplers were fastened to a 46-meter metal tower which was installed approximately 20 meters northeast of the reactor. The remaining samplers were placed on a nylon line fastened to the top of the 46-meter IET stack located approximately 75 meters north of the reactor.

The vertical distribution of the airborne release was monitored by ten high-volume air samplers, fifteen fallout plates, and fifteen film badge dosimeters that were evenly spaced from the ground to the top of the 46-meter tower. One recording-type remote radiation detector also was located at the 23-meter level on the tower. Fourteen fallout plates and fourteen film-badge dosimeters were evenly spaced on the line connected to the top of the IET stack.

5.2 "Clothesline" Device

To avoid excessive exposure during the early recovery of samples located near the reactor, a "clothesline" device with pulleys was constructed. One pulley attachment was tied to the reactor superstructure approximately 3.5 meters above the reactor core, and a second pulley was anchored 61 meters east of the test pad. With this arrangement, samples could be positioned and then recovered by a recovery team at the end of the 61-meter clothesline. This system was used to position two nuclear accident dosimeters (Hurst Threshold Detectors), two NRTS film badges, a section of copper wire, an activation foil box, a sample of human hair, and a high range gamma dosimeter. These devices were positioned above the reactor where they would be exposed directly to the reactor core.

5.3 Air Support

In addition to the instruments in fixed locations, aerial monitoring and mobile monitoring units were used to estimate the intensity, travel, and dispersion of the radioactive cloud.

Air support for the destructive test was provided by ID Health and Safety Division. An airplane, equipped with radiological monitoring instruments, was used prior to the test to confirm that downwind restricted areas were cleared of vehicles and personnel. Following the test, the aircraft was used to locate and follow the radioactive cloud as it passed beyond the monitoring grid and the boundaries of the testing station.

5.4 Telemetering Network

Two telemetering systems were used in conjunction with the destructive test. One system, operated by Phillips Petroleum Co. Health and Safety, consisted of 25 station units (Figure 14) which reported by radio to a central control panel

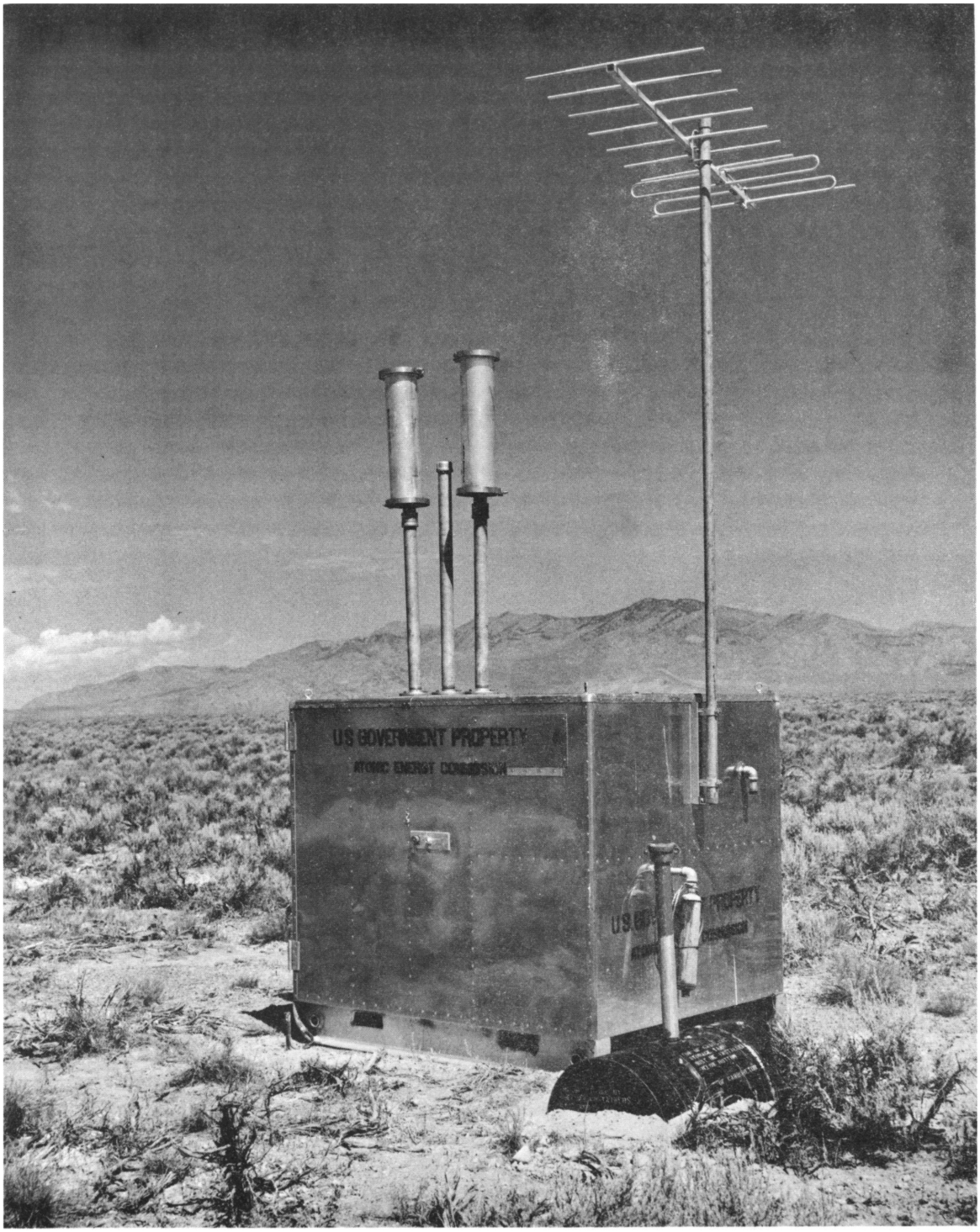

Fig. 14 Remote telemetering station.

located in the Test Area North, Health Physics Laboratory. This network was designed to measure and immediately report the gamma dose rate and the amount of gross airborne particulate activity near ground level from a radioactive cloud.

The second system, operated by ID Health and Safety, consisted of 6 station units from the ID Health and Safety radio-telemetry radiation monitoring network. These units report by radio to the control panel in the ID Health and Safety Laboratory. Each of the station units contained an ion chamber and an air sampling system for measuring particulate activity collected on a filter and gaseous and iodine activity collected on a charcoal trap.

III. TEST OPERATION

Following four full scale "dry-runs", a change in the month-long weather pattern over the Western United States permitted the U. S. Weather Bureau to issue a favorable weather forecast for operation of the destructive test on April 1, 1964. Count down procedures for preparation of the radiological monitoring network were started at 0600 hours on April 1. Field crews from each of the three monitoring organizations drove to their assigned areas and began preparing the sampling stations for the test. Portable generators and high- and low-volume air samplers were started, fallout plates and film-badge dosimeters were placed in test position, and other sampling devices, such as water catch cans and fission-gas detectors, were made ready at their respective locations. Monitoring trailers, which also served as communication control centers, were placed at the edge of the 60° sector of the grid in preparation for receiving and dispatching samples recovered from the grid following the test. Each responsible group had two-way radio contact between field crews, reactor test personnel, and their respective control centers. By 1030 hours, all grid stations had been activated and the Phillips Petroleum Co. Health and Safety controlled portion of the grid area was cleared of personnel. Count down procedures continued without incident until 1144 hours, when the destructive excursion was initiated.

Within milliseconds following the initiation of the reactor excursion, steam and water were ejected from the environmental tank in a spherically shaped cloud. The cloud maintained its symmetrical shape for a short time during which most of the water collapsed back into the environmental tank. Following the collapse of the water, a visible, vapor-filled cloud blew downwind over the heavily instrumented sector of the monitoring grid. Telemetered data from the 2500-meter arc provided immediate information that the radioactivity release had been small and that no significant radiation hazard had been created.

Following the destructive excursion, the senior staff of the Engineering and Test Branch evaluated the condition of the reactor using TV cameras, water level indicators, and nuclear radiation detectors to determine that the reactor remains were in a safely shutdown condition. Approval was given for the reentry team to enter the test cell area at 1220 hours. The first reentry team, consisting of a reactor engineer, a surveillant physicist, and a health physicist, entered the test cell area at approximately 1223 hours. Direct radiation readings reported by the health physicist were as follows (see Figure 15 for dose-rate reading locations at their respective shielded locations): 0.2 mrem/hr in the IET change room, 50 mrem/hr at the corridor shielding door, 150 mrem/hr at the test cell entrance, and 400 mrem/hr on the test pad adjacent to the environmental tank. The team made a brief inspection of the test area and the environmental tank and returned to the underground change room where they were surveyed for contamination. Low level activity (< 1.0 mrem/hr) was detected by a GM portable survey instrument on the soles of the shoe covers worn by the reentry team, which indicated that the reactor test pad was only slightly contaminated.

At approximately 1240 hours, sample recovery teams, carrying portable radios, began retrieving samples from the radiological grid and from around the reactor test pad. Radio-equipped vehicles were used on the grid for sample recovery. To gather release data and for personnel protection, two of the

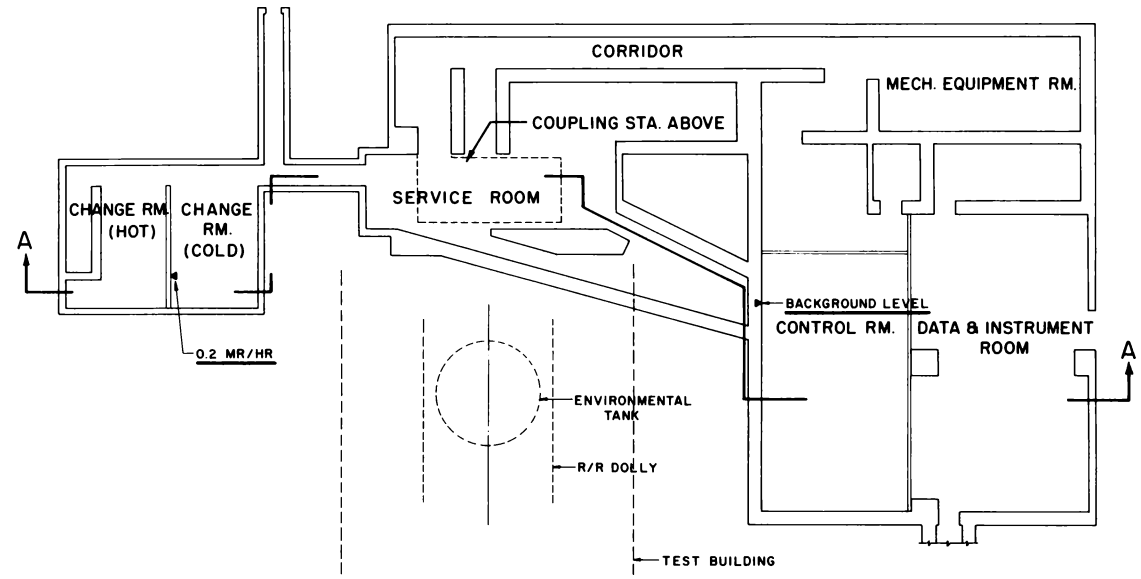

FLOOR PLAN

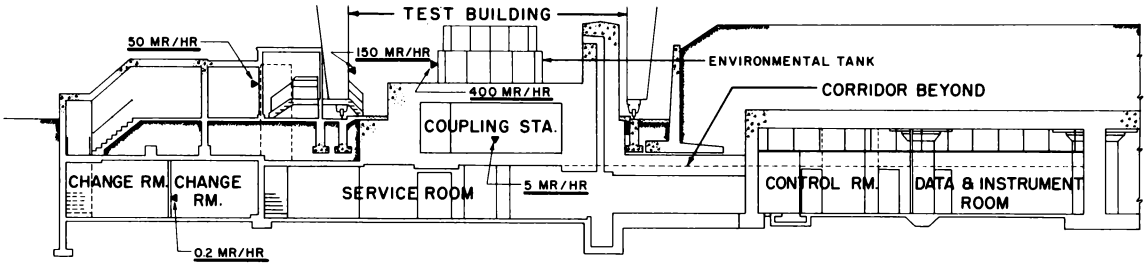

SECTION A-A

Fig. 15 Layout and cross section of the IET test area.

vehicles were equipped with air monitoring and direct radiation measuring instrumentation. All samples to be analyzed for short-lived activity were collected by 2000 hours. Other nonpriority samples were collected the following day. Samples collected from the grid were checked through the sample recovery trailers, sealed in plastic bags, and routed to those responsible for the analyses.

IV. PRESENTATION OF DATA

The data obtained from the test have been divided into three general groups: (a) fission-product-release data, (b) direct radiation dose and dose rate data, and (c) meteorological data.

1. FISSION-PRODUCT DISTRIBUTION

Fission products from the test were distributed among the radioactive cloud, the water in the environmental tank, and the solid remains of the reactor fuel. Measurements were made on each of these three items in order to determine the isotopic distribution of the fission products from the test.

1.1 Radioactive Cloud

1.11 Description. Water and steam were ejected in a spherical cloud directly above the environmental tank. The cloud maintained its spherical shape for several seconds despite the 20-mph wind blowing at the time of the test [1]. Most of the water fell back into the environmental tank; after which a visible, vapor-filled cloud was blown downwind. A second vapor cloud arose from the tank following the collapse of the water. This second cloud merged with the first by the time they reached the 25-meter arc. Movies taken of the test show the vapor height at the 25-meter arc to be approximately 12 meters.

The monitoring airplane intercepted the main cloud at approximately one mile from the test site and followed it for twenty-one miles before cloud dispersion and radioactive decay reduced the radiation levels to background. At eleven miles from the test site, the airplane measured a peak reading of 0.1 mrem/hr while flying at approximately 1200 feet above the terrain.

Samplers and mobile surveillance teams, positioned at locations greater than one mile downwind, gave indications as to the size of the cloud at several distances, as shown in Table I.

TABLE I

CLOUD SIZE VERSUS DISTANCE

Downwind Distance	Cloud Width	Cloud Passage Time
1.5 miles	2100 ft	30-45 sec
2.5 miles	3120 ft	1.5 min
5.5 miles	Unknown	3.0 min
11.0 miles	2 miles	Unknown

1.12 Cloud Fission Products. Only daughters of noble fission gases (3-sec Kr-92, 10-sec Kr-91, 16-sec Xe-140, and 41-sec Xe-139) were collected by air sampler filters. In addition, the barium daughter of Xe-139 was also detected on charcoal cartridges in the air samplers, and the cesium daughter of Xe-138 was collected by a fission-gas detector designed to hold the relatively longer lived gases for decay. Table II on the following page lists the type of sample, grid location (Figures 4, 5, 6, and 7), and the activity collected by all samplers that retained sufficient activity for quantitative analysis.

TABLE II

AIR SAMPLER FILTER DATA
(Activity corrected to 1400 hours, April 1, 1964)

Sample Location	9.7 hr Sr-91 (μc)	2.7 hr Sr-92 (μc)	85 min Ba-139 (μc)
A-3	0.351	0.324	0.227
A-4	0.73	0.70	0.951
B-3	0.294	0.30	0.432
B-5	0.108	---	---
C-8	0.503	0.191	1.28
C-9	0.0035	---	---
D-7	0.0038	---	---
D-8	0.206	0.164	0.241
E-16	0.034	0.028	0.049
F-18	0.0216	0.01	0.016
F-20	0.029	0.024	0.043
G-12	0.0013	---	---
G-13	0.0019	---	---
G-15	0.014	0.0096	0.019
H-10	0.0035	---	---
H-11	0.0124	0.0097	0.023
H-12	0.016	0.013	0.028
J-9	0.0019	0.0015	0.0031
J-13	0.0096	0.0077	0.016
J-15	0.0022	0.0018	0.0037
K-9	0.001	0.00084	0.0017
K-11	0.0023	0.0018	0.0038
K-13	0.0034	0.0027	0.0057
K-15	0.00072	0.00058	0.0012
L-11	0.00015	0.00012	0.00025
L-13	0.0021	0.0017	0.0034
L-15	0.0015	0.0012	0.0025
L-17	0.00032	0.00026	0.00053
Tower (15 feet high)	1.36	1.44	0.443
Tower (30 feet high)	0.516	0.519	0.194

TABLE II (cont.)

AIR SAMPLER FILTER DATA
(Activity corrected to 1400 hours, April 1, 1964)

Charcoal Cartridges from High-Volume Air Samplers

Sample Location	9.7 hr Sr-91 (μc)	2.7 hr Sr-92 (μc)	85 min Ba-139 (μc)
A-3	0.0067	0.0047	0.0196
A-4	0.016	0.014	0.113
C-8	0.0074	0.006	0.04

Fission-Gas Detector

Sample Location	32 min Cs-138 (μc)
A-3	0.063

1.13 Cloud Volume. Although the volume of the radioactive cloud was constantly changing because of diffusion, it is of some interest to estimate its volume at the 25-meter (A) arc where the radiological tower provided a vertical measurement of the cloud height.

The length of the visible cloud was calculated from motion picture data, which showed that it took the cloud approximately ten seconds to move past the radiological tower. Weather data at this time showed a wind speed of 25 mph. Combining these two facts, the cloud length passing the radiological tower was calculated to be 110 meters.

An upper limit on the height of the cloud was determined by visual inspection of the motion pictures and by beta film-dosimeter readings. Because of the short range of beta particles in air, beta activity, measured by film dosimeters, would indicate that the cloud had passed near the film-badge location. Both of these determinations indicate that the top of the cloud at the 25-meter arc was approximately 12 meters.

The width of the cloud could only be bracketed with the data obtained from the test. Radioactive particulates were detected on the high-volume air samplers stationed at the A-3 and -4 positions, showing that the cloud passed over these stations. The absence of activity on the filter from positions A-2 and -5 indicated that the cloud was not wide enough to reach these stations. Since these stations are located approximately 13 meters apart, it is estimated that the maximum width of the cloud at the (A) arc was on the order of 30 meters.

Using these bracketing figures, an upper limit of the cloud volume as it passed the (A) arc was calculated to be 4.13×10^4 cubic meters.

1.2 Fission Products In Water

During the first five minutes following the test, most of the water from the environmental tank was rapidly drained to an underground hot waste storage tank to prevent a secondary criticality from the reactor debris. A sampling system, designed to obtain samples from this water as it flowed to the waste storage tanks, failed to function properly; therefore, samples of the environmental tank water were obtained from the hot waste storage tank two days following the test. Samples of the water expelled during the excursion were captured in catch cans and in five of the water trays located outside the reactor environmental tank. The fission product activity, detected in the water from the test, was determined by radiochemical analysis and the isotopic concentration found in the different samples is shown in Table III.

TABLE III

WATER ANALYSIS DATA
(μc/ml at 1400 hours, April 1, 1964)

	Isotope				
Sample	Ce-141	I-131	Ba-La-140	Zr-Nb-95	Ru-103
Waste Tank	9.06×10^{-6}	1.36×10^{-4}	No Analysis	1.64×10^{-6}	No Analysis
Tray 1	3.2×10^{-4}	$< 1.07 \times 10^{-5}$	3.5×10^{-4}	4.77×10^{-5}	1.35×10^{-4}
Tray 2	2.13×10^{-4}	None	3.34×10^{-4}	1.30×10^{-5}	None
Tray 3	2.86×10^{-4}	$< 5.92 \times 10^{-6}$	3.01×10^{-4}	1.41×10^{-5}	None
Tray 4	2.76×10^{-4}	None	2.85×10^{-4}	1.26×10^{-5}	None
Tray 5	7.59×10^{-5}	$< 2.33 \times 10^{-6}$	None	6.69×10^{-6}	None
Catch Can					
2-1	[a]	[a]	[a]	[a]	[a]
2-2	8.82×10^{-4}	Background	Background	Background	6.95×10^{-4}
2-3	1.45×10^{-5}	9.63×10^{-6}	Background	Background	Background
2-4	[a]	[a]	[a]	[a]	[a]
2-5	8.15×10^{-5}	7.82×10^{-5}	1.60×10^{-4}	5.32×10^{-5}	3.37×10^{-5}
2-6	5.62×10^{-6}	7.34×10^{-6}	9.32×10^{-6}	2.02×10^{-6}	4.82×10^{-6}
2-7	Background	1.48×10^{-4}	Background	Background	Background
2-8	7.35×10^{-7}	Background	Background	Background	2.54×10^{-6}
2-9	Background	1.35×10^{-6}	Background	Background	Background
2-10	1.23×10^{-5}	Background	Background	Background	Background
2-11	4.12×10^{-6}	9.93×10^{-6}	Background	Background	Background
2-12	1.04×10^{-6}	$< 4.04 \times 10^{-6}$	Background	Background	Background

[a] Insufficient for analysis.

In addition to the isotopes listed in Table III, large quantities of activated sodium (Na-24) and trace quantities of Ce-143, Np-239, Te-132, I-132, and I-133 were detected in the environmental tank water.

Of the 10,000 gallons of water originally in the tank, all but about 500 gallons returned to the tank following the initial power burst.

1.3 Fuel Analysis

1.31 Radiochemical Analysis for Fission Products. Because of the problems connected with recovering radioactive fuel and in preparing suitable sample specimens for radiochemical analysis, the fuel analysis was not started until nearly one month following the test. Because of this relatively long time interval, only the longer-lived isotopes could be quantitatively determined by radiochemical analysis. The fission-product distribution in four samples from each of three fuel pin remains is shown in Table IV.

TABLE IV

FUEL ANALYSIS DATA
(Expressed as μc/gm at 1400 hours, April 1, 1964)

Fuel Pin Sample Number	I-131	Ba-La-140	Ce-141	Zr-Nb-95	Cs-137	Sr-89
65-1	16	24	3.3	4.3	0.026	4.7
65-2	23	47	5.9	9.1	0.049	8.8
65-3	8	44	6.1	9.2	0.057	8.4
65-4	23	23	1.3	4.2	0.029	3.5
151-1	10	25	2.5	4.8	0.025	4.6
151-2	22	39	3.6	7.8	0.046	7.3
151-3	27	46	4.5	9.1	0.057	8.1
151-4	15	23	2.4	4.4	0.028	4.5
153-1	15	21	2.1	4.1	0.024	3.8
153-2	17	34	3.4	6.7	0.036	5.8
153-3	12	34	4.0	8.0	0.026	6.6
153-4	---------- Lost Sample ----------					

Since it appeared that only a small percentage of the noble gases was released to the atmosphere, analytical efforts to determine the fraction remaining in the fuel were initiated. Krypton-85 was selected for the noble gas analysis because its 10.4 year half-life was sufficiently long that only minor corrections were required for losses due to radioactive decay. On July 26, 1964, 86 days following the test, $3.90 \times 10^{-3} \pm 50$ percent μc of Kr-85 per gram of fuel was detected in sample wafers from fuel pin E-147.

1.32 Fragmentation and Fuel Temperature. Both the fuel surface area and temperature affect the release of fission products. The more finely divided fuel fragments, with their corresponding larger surface area, would be expected to release more fission products than the larger, intact segments. Likewise, the temperature reached by the fuel would have a considerable effect on the quantity of the volatile fission products vaporized from the fuel. These two factors are not completely independent because the fragmentation of the fuel was the result of the intense pressures generated by hydrogen, freed from the hydrided fuel; and the quantity of hydrogen, freed from the fuel, is related to the fuel temperature. The maximum core-averaged fuel temperature was 1900 ± 200°F [1]. Figures 16 and 17 show the identifiable remains of the 37 fuel rods; the largest

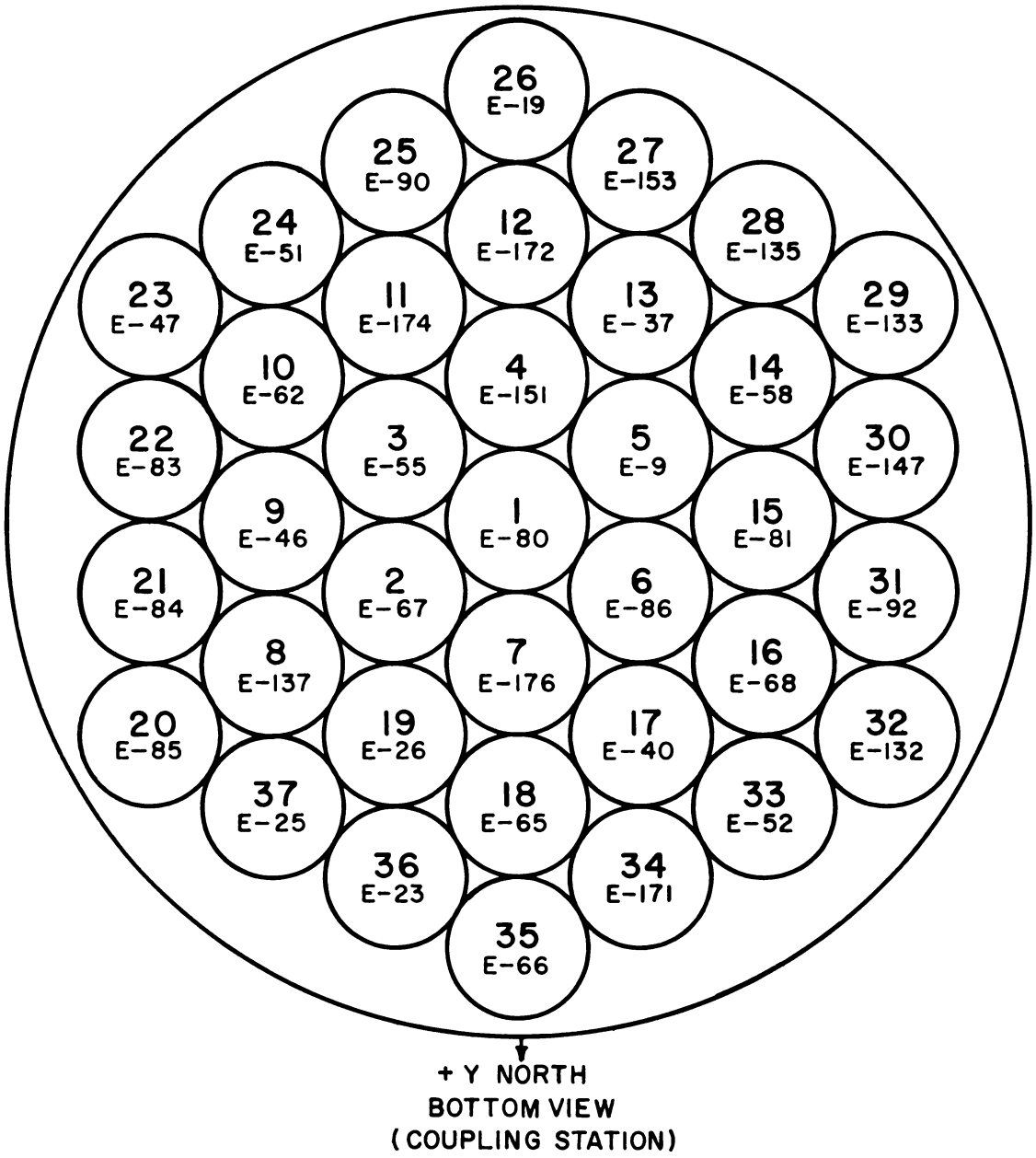

Fig. 16 SNAPTRAN 2/10A-3 core layout.

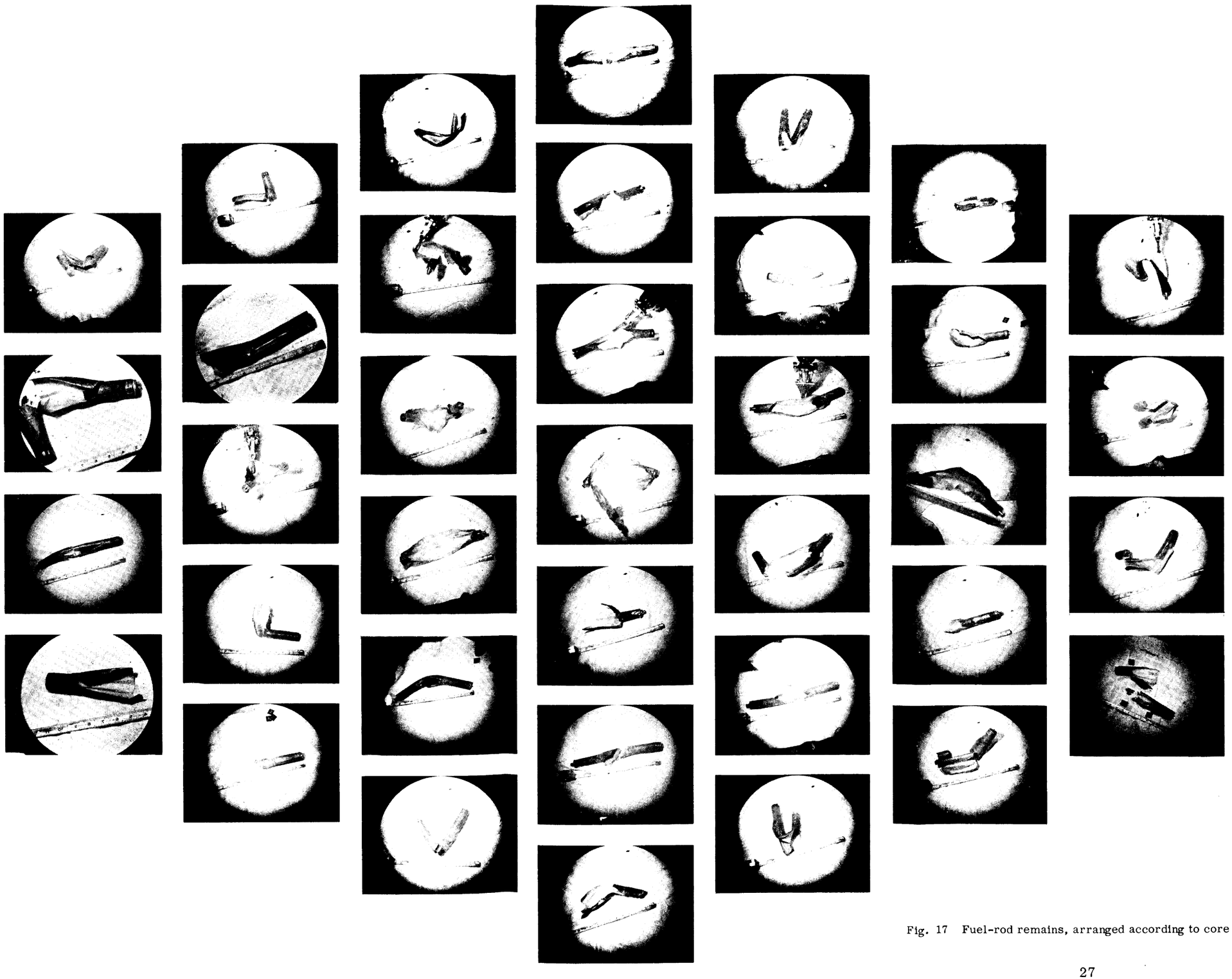

Fig. 17 Fuel-rod remains, arranged according to core layout.

intact pieces, between 3 and 4 inches long, were from outer fuel rods. The fuel from the center pin was completely expelled from the fuel cladding. Table V shows the approximate size range of the fuel following the test.

TABLE V

FUEL PARTICLE SIZE RANGE

Particle Size Range	Grams[a]		
Less 74 microns	13.0		
74 to 149 microns	74.9		
149 to 1,000 microns	1,015.17		
1,000 to 4,760 microns	2,776.0		
Greater 4,760 microns	53,335.93	Total Grams Prior to Test	Percent Recovered
Total	57,215.00	57,720	99.2

[a] Includes fuel, cladding, and end caps.

2. DIRECT RADIATION MEASUREMENTS

The direct radiation resulting from the excursion, the residual fission products, and the radioactive cloud was monitored by both remote radiation monitors and film-badge dosimeters. Unexpectedly low readings in some areas can, for the most part, be explained by various amounts of shielding between the film dosimeter and the reactor.

2.1 Excursion Prompt Radiation

2.11 Gamma Radiation. A remote radiation monitor with a 1000 R/hr gamma detector was located on the edge of the environmental tank. The reading from this monitor went off scale at the instant of the power burst, after which the instrument failed as it was deluged by water and debris from the environmental tank. A remote radiation monitor, 6.1 meters directly west of the reactor where it was shielded by the environmental tank, gave a peak reading of 30 rem/hr. However, because of their relatively long time constants, these instruments were unable to follow the high-intensity, short-duration power burst, and their readings are low. Detectors with extremely short response times, recording on magnetic tape recorders, were able to follow the dose rate from the prompt excursion radiation, and a graph of the dose rate versus time from one of the detectors is shown in Figure 18. The peak burst dose rate, recorded by this detector through 43 inches of water, was 1.8×10^8 rem/hr. The total integrated dose obtained by integrating under the dose-rate curve was 128 rem.

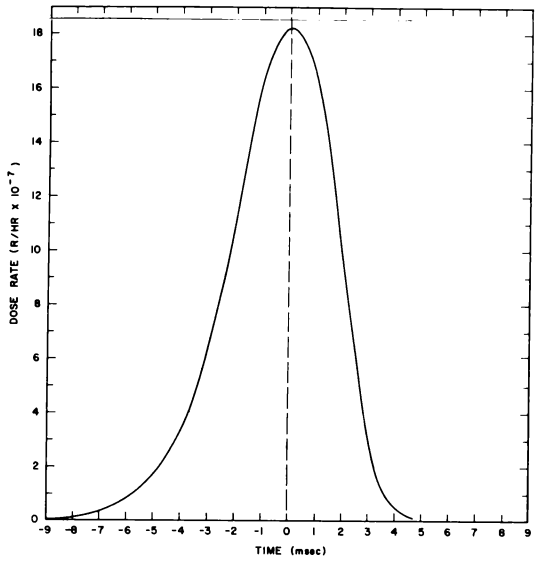

Fig. 18 Prompt gamma dose rate from excursion.

2.12 Neutron Radiation. During the power burst, neutrons were expelled to the immediate environment. These were measured by Hurst nuclear accident dosimeters and biological samples. Table VI summarizes the information received from the neutron-detection mechanisms.

2.2 Fission-Product Delayed Radiation

The remote radiation monitor, 6.1 meters to the west of the reactor, indicated a radiation field of 55 mrem/hr, 120 minutes after the test. Twenty-four hours later this same chamber indicated a radiation field of 2 mrem/hr.

The measured film-badge-dose results from direct radiation on or near the environmental tank are indicated at their respective locations in Figure 19. The average gamma doses recorded by these groups of film badges with similar locations and exposure times are shown in Table VII.

2.3 Cloud Radiation

Direct radiation from the cloud was measured by remote radiation monitors, film dosimeters, and film dosimeters located in "wells". The downwind film-dosimeter exposures indicate that the cloud passed down the center of the grid directly over the five remote radiation monitors located on the centerline of the 60° sector of the radiological grid. The dose rates measured by these monitors are considered to be the maximum from the cloud at each arc. The measured dose rates from the detectors are shown as a function of time and distance in Figure 20. The traces show a small response to the "burst" radiation, followed by a decay of the delayed gamma radiation prior to the arrival of the cloud.

Within 100 meters of the reactor, the integrated dose, recorded on film-badge dosimeters, was due to direct radiation from the reactor as well as from the cloud. The "well" film dosimeters, being shielded from the reactor, saw only the direct radiation from the cloud. As shown in Table VIII and Figure 21, the maximum recorded radiation dose from the cloud occurred within 25 meters of the reactor. Three stations on the 25-meter arc recorded total beta-gamma doses of 240 mrem, 460 mrem, and 290 mrem, respectively. One hundred meters from the reactor, the maximum dose from the cloud, as measured by a "well" film-badge dosimeter, was 35 mrem. Cloud dispersion and radioactive decay were such that film dosimeters at all grid stations, 300 meters or more from the reactor, recorded less than 25 mrem, total dose.

2.4 Film Dosimeters on the Grid

The radiation from the power burst, residual fission products, and the radioactive cloud was insufficient to give positive readings on the film dosimeters at most positions on the grid. Those that did show significant readings are listed in Table VIII.

TABLE VI

NEUTRON MEASUREMENTS

Position of Detector	Activation and Fission Material	Integrated Thermal Flux (n/cm^2)	Integrated Fast Flux (n/cm^2)	Total Integrated Dose (rads)
NAD #1 -- Five feet above reactor	Gold	6.5×10^7		
	Plutonium		> 1 KeV = 3.7×10^{10}	
	Neptunium		> 0.75 MeV = 5.0×10^{10}	0.7
	Uranium		> 1.5 MeV = 6.6×10^{10}	
	Sulfur		> 2.5 MeV ≈ 0	
NAD #2 -- Seven feet above reactor	Gold	6.5×10^7	Not analyzed, Similar to NAD #1	
	Plutonium			
	Neptunium			
	Uranium			
	Sulfur			
NAD #3 -- On camera dolly	Gold	4.0×10^7	Not analyzed,	
	Plutonium		Equipment failure	
	Neptunium			
	Uranium			
	Sulfur			
NAD #4 -- 25-m Arc	Gold	No Activation		
	Plutonium			
	Neptunium			
	Uranium			
	Sulfur			
NAD #5 -- 50-m Arc	Gold	No Activation		
	Plutonium			
	Neptunium			
	Uranium			
	Sulfur			
NAD #6 100-m Arc	Gold	No Activation		
	Plutonium			
	Neptunium			
	Uranium			
	Sulfur			
Copper Wire -- Five feet above reactor	Copper	Recovered too late for analysis $T_{\frac{1}{2}}$ Cu-64 = 12.9 hr		
Hair Sample -- Five feet above reactor	Sulfur	No Activation		
Film Badge -- EGG dolly	Indium			
	Gold			
	Cadmium covered Gold	7.3×10^7		
Blood Sample -- EGG dolly	Sodium	Assumed same neutron spectra as NAD #1		0.7

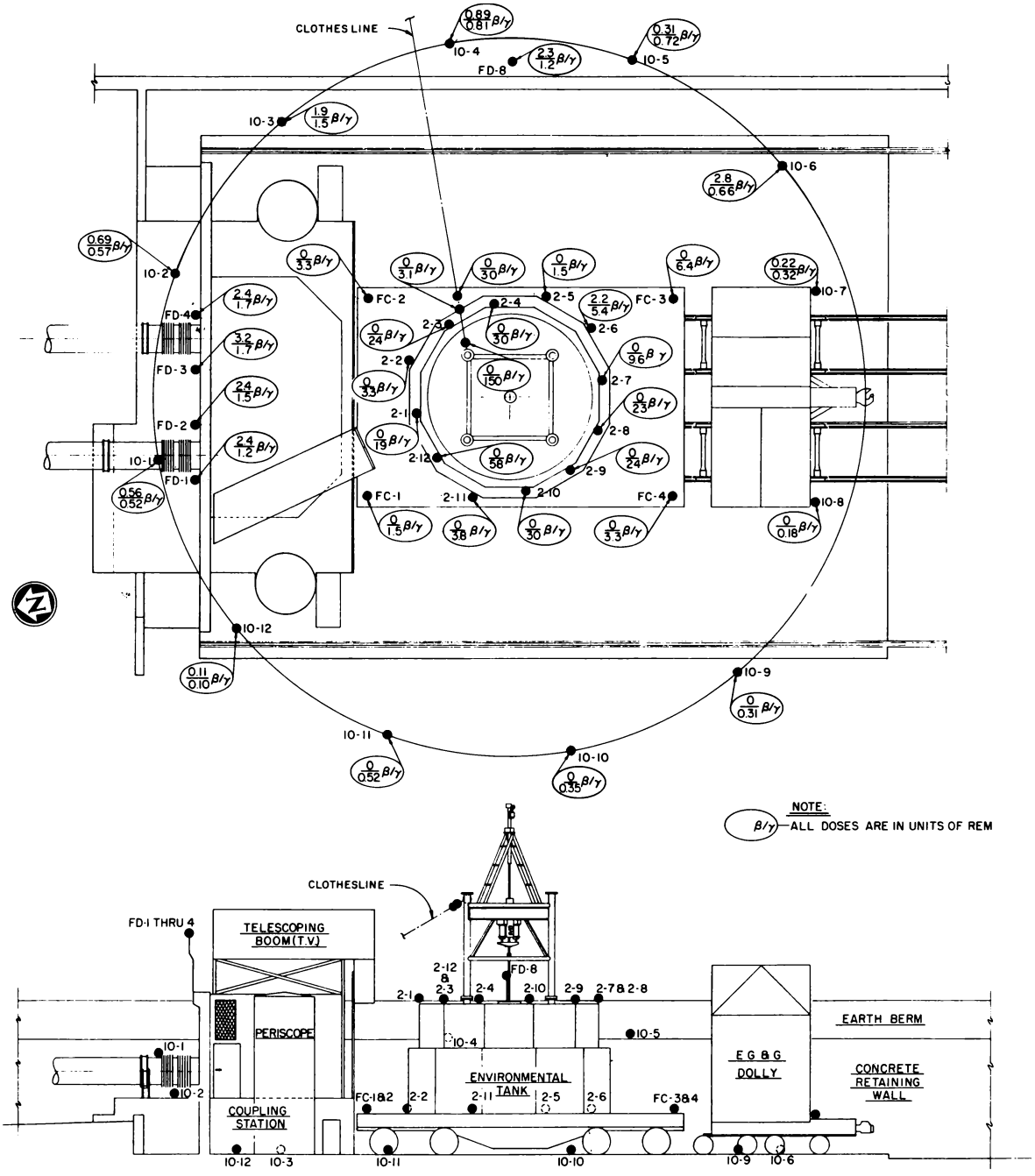

Fig. 19 Dose measurements on and around environmental tank.

TABLE VII

RADIOLOGICAL MEASUREMENTS INSIDE TEST CELL AREA

Location	Approximate Exposure Time (hr)	Average Dose (rem)
Top of Tank	24	38
On Dolly next to Tank	24	3.5
Corner of Reactor Dolly	24	3.6
On EGG Dolly	1/2	0.25
North End of Test Cell	24	1.5
10-Meter Arc	24	0.70
10-Meter Arc	3	0.39

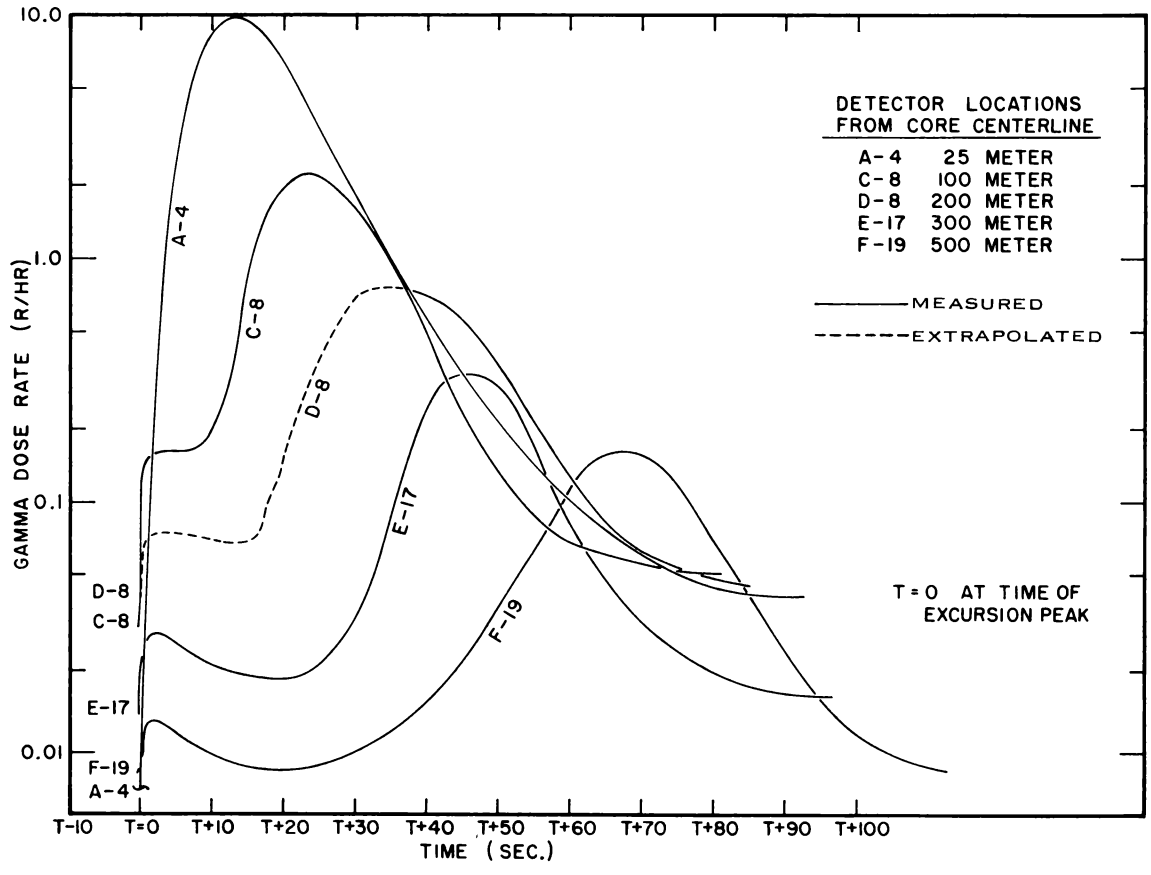

Fig. 20 Cloud dose rate measurements at downwind locations.

TABLE VIII

GRID FILM-DOSIMETER DATA

Film Dosimeter Location	Gamma Reading (mrem)	Beta Reading (mrem)
A-1	130	100
A-2	130	0
A-3	115	450
A-4	170	850
A-5	195	800
A-6	180	270
A-7	90	220
A-8	115	150
A-9	60	0
A-10	65	150
A-11	80	120
A-12	95	0
B-1	15	60
B-2	10	60
B-3	30	70
B-4	140	500
B-5	15	0
B-6	25	0
B-7	20	0
B-8	50	30
B-9	35	0
B-10	50	30
B-11	25	60
B-12	50	50
C-8	30	250
D-8	45	0
E-18	25	0
F-18	40	0
A-3 Well	50	190
A-5 Well	30	260
B-4 Well	75	0
B-5 Well	0	0
C-7 Well	0	0
C-8 Well	35	0
C-9 Well	0	0

2.5 Film Dosimeters on the Radiological Tower

The measured doses, recorded by film dosimeters on the radiological tower, which was located about 65 feet downwind from the reactor, are shown as a function of tower height in Figure 22. These badges were retrieved approximately 5 hours after the test. The gamma readings reflect the exposure from the reactor and the cloud. The beta readings reflect radiation from the cloud only, with the shape of the curve indicating two different levels of activity in one cloud or two separate clouds with different heights.

2.6 Dosimeters Other Than Film Dosimeters

In addition to the film dosimeters, there were several other high range dosimeters located near the reactor. Their measured dose results are shown in Table IX. The location notations correspond to the positions indicated in Figure 19. Because of the low radiation doses from the reactor, most of these dosimeters were exposed below their minimum applicable ranges.

2.7 Phantom Doses

The film badges placed on the standard-man phantoms provided dose measurements at several locations near the reactor and also provided information about their use for accident dose measurements. Each phantom was circled with a belt of twelve badges to determine the effect of badge orientation with respect to the radiation from a reactor excursion. Figure 23 shows the variation in dose measurement as a function of badge position on the phantom. The badge, numbered as 12, faced the reactor; badges 3 and 9 were essentially parallel to the radiation beam; and badge 6 was on the back side of the phantom. In addition, the doses measured by the two badges, suspended in air below the phantom, and the depth dose, measured by the badge suspended within the phantom's tissue-equivalent solution, are indicated in the figure.

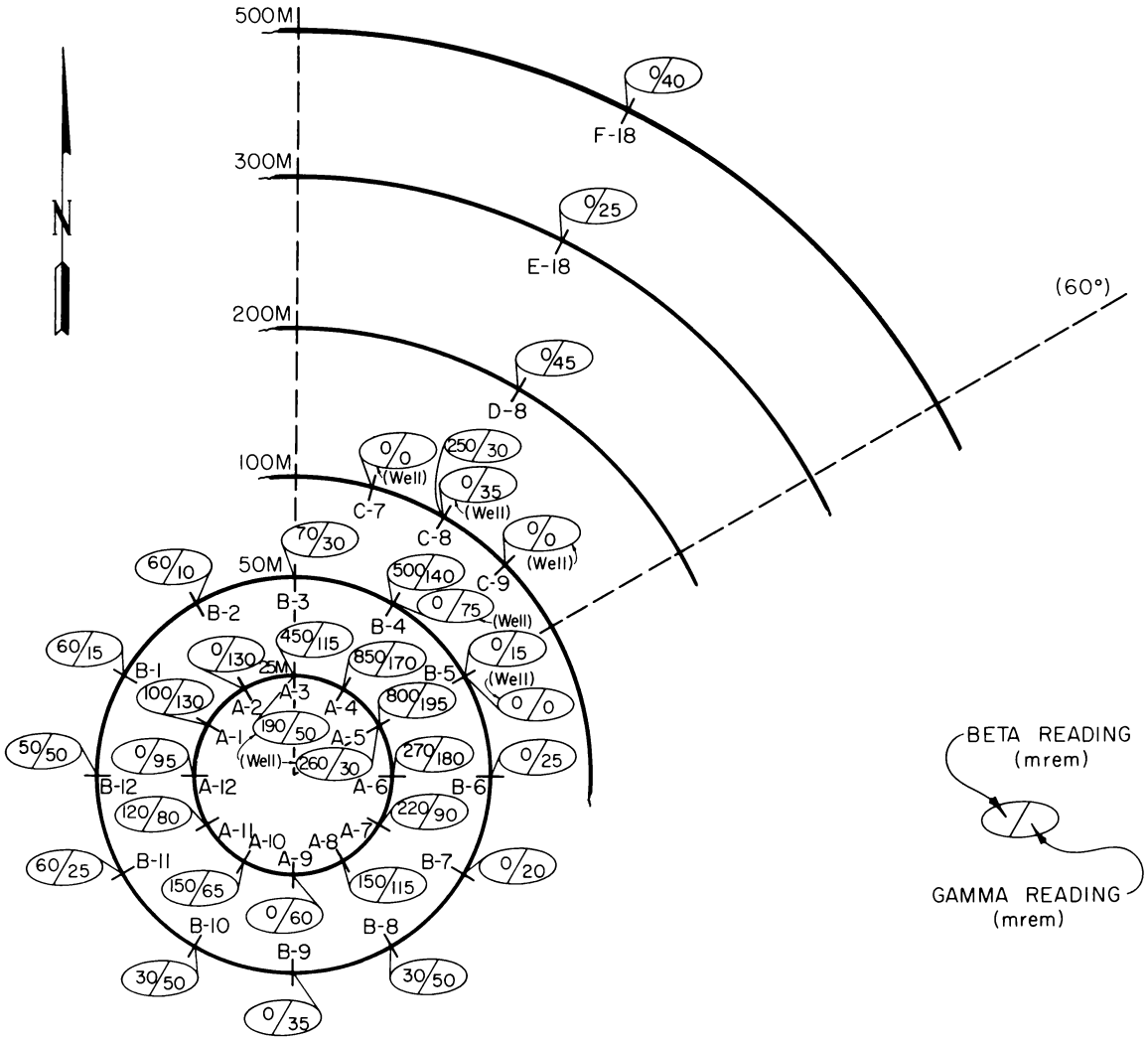

Fig. 21 Grid radiological dose measurements.

3. BERYLLIUM RELEASE

Emission spectra analysis of high-volume air-sampler filters, fallout plates, and filters from the water catch cans showed only background levels of beryllium, indicating that beryllium was not released from the reactor. Subsequent visual examination of the beryllium reflector pieces showed that they had not fractured into small pieces. The main damage was restricted to the breaking of a 6 x 12 inch piece in half.

4. METEOROLOGICAL PARAMETERS

A few sprinkles of rain were observed over the southern part of the NRTS on the morning of the test, and general shower activity occurred in eastern

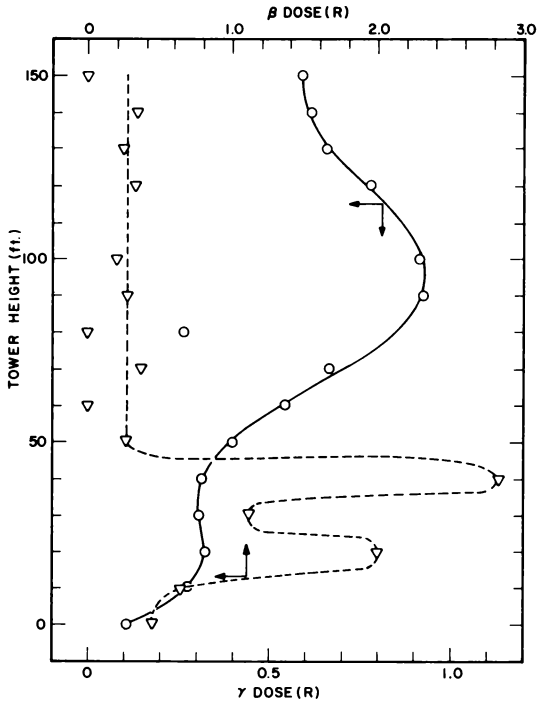

Fig. 22 Dose measurements from radiological tower locations.

Idaho. Favorable wind and stability conditions were established over the test grid by 1015 hours on April 1, 1964. Cloud cover varied from broken to overcast and was forecast to thicken and lower. At 1144 hours, the destructive test was initiated. The cloud cover at TAN was broken; the atmospheric condition was slightly unstable, allowing good diffusion; and the wind, measured instantaneously at the 46-meter level at IET, had a direction of 205 degrees and a speed of 25 miles per hour. The mean wind direction and speed over the grid and downwind of the IET are summarized in Table X.

The temperature differential between the 61-meter height and the 1.5-meter height was $\Delta T = -1.4°C$. The test, therefore, was conducted under slightly unstable atmospheric conditions. The winds were extremely steady with little thermal turbulence because of the cloud cover. The horizontal and vertical wind direction standard deviations, σ_θ and σ_ϕ, are listed in Table XI, along with the wind speed standard deviation, σ_u. The table also indicates the estimated vertical and horizontal cloud spread parameters, σ_z and σ_y, as a function of distance.

The σ_y value was obtained from the air sample measurements on the test grid (Appendix A), and σ_z has been estimated relative to σ_y, according to previous 30-minute diffusion measurements at the NRTS.

The vertical growth of the radioactive cloud was not measured, so that the distance dependency of σ_z was not determined. The estimated peak concentration values, obtained from the air sample measurements, did not satisfactorily define the overall cloud growth. However, the growth appeared to be less than would be predicted by Sutton or by Pasquill Class-C (Reference A-3) parameters, for slight atmospheric instability, which are based on effluent release times of several minutes.

TABLE IX

HIGH RANGE DOSIMETER DATA

Kind of Dosimeter	Location	Approximate Time of Exposure (hr)	Gamma Dose (rem)
Glass Rod	2-1	24	39 ± 1
	2-3	24	30 ± 2
	10-1	24	< 25
	10-3	24	< 85
	10-5	24	< 25
	10-7	24	< 25
	10-9	3	< 25
	10-11	3	< 25
Chemical	FC-1	24	< 50
	FC-2	24	< 50
	FC-3	24	< 50
	FC-4	24	< 50
	2-2	24	< 50
	2-4	24	< 50
	2-6	24	< 50
	2-8	24	< 50
	2-10	24	< 50
	2-12	24	< 50
	10-2	24	< 25
	10-6	24	< 25
	10-8	24	< 25
	10-10	3	< 25
	10-12	24	< 25
Thermoluminescent	On clothesline above tank	1	52
	On EGG dolly	< 1/2	0.79

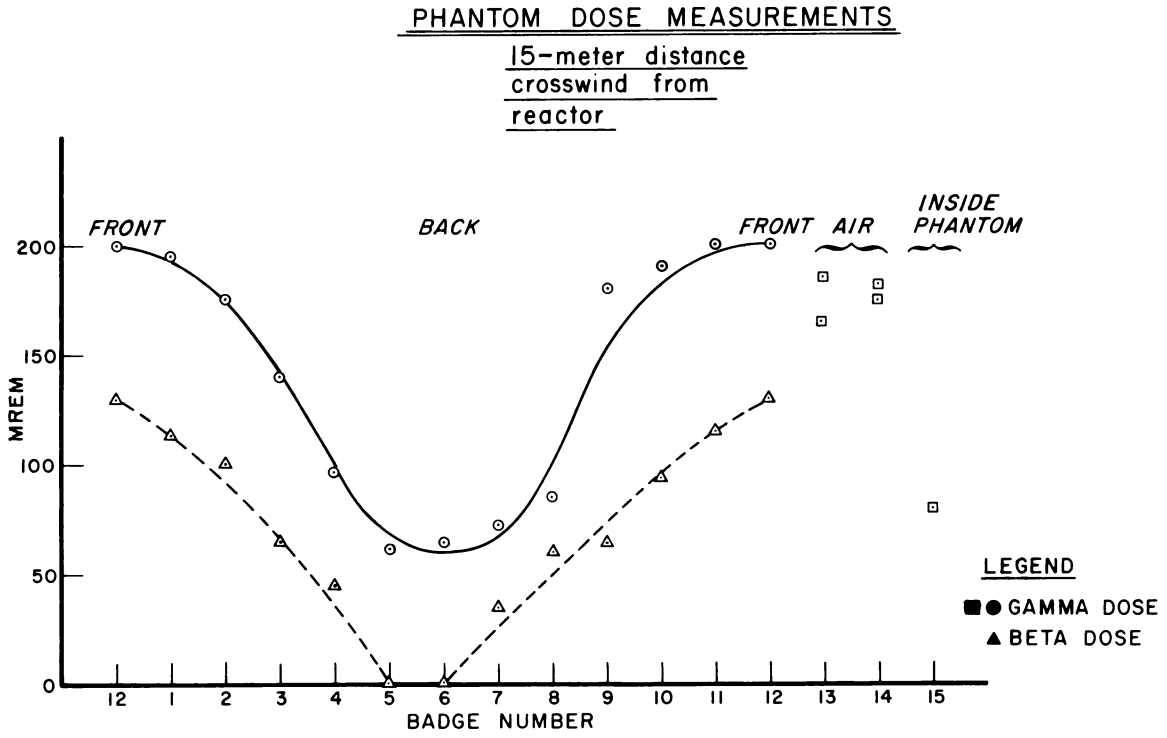

Fig. 23 Phantom film-dosimeter results.

TABLE X

METEOROLOGICAL PARAMETERS

Instrument	Mean Directions and Speeds During the Test	
	Direction (degrees)	Speed (mph)
IET 20 feet	203	22.2
IET 200 feet	208	25.5
Station 179	209	17.7
Station Monteview	197	18.6
Tetroon (released after test)	209	27.9

TABLE XI

TURBULENCE AND DIFFUSION PARAMETERS[a]

	6.1-Meter Height	61-Meter Height
σ_θ (degrees)	6.7	3.4
σ_ϕ (degrees)	3.2	3.1
σ_μ (m/sec)	1.0	0.5
$\sigma_y = 0.20x^{0.85}$		
$\sigma_z = 2/3\ \sigma_y$, for short distances, x		

[a] Three minutes sampling time -- four seconds averaging time.

V. DATA ANALYSIS

A number of important conclusions can be drawn from the destructive test data; some of which, including the distribution of radioactive iodine, the fraction of fission products released to the atmosphere, and the success of analytical models in predicting direct radiation doses, are explored in this section.

1. IODINE DISTRIBUTION

Because of its potential biological hazard, a great deal of interest has been shown in the release of iodine from damaged reactor fuels, especially in fuels which have been ruptured under accident conditions. For this reason, an attempt was made to account for the iodine produced during the SNAPTRAN 2/10A-3 destructive test.

1.1 Available Iodine

The number of curies of various iodine isotopes which were produced during the destructive excursion and were, therefore, available for release to the atmosphere at the time of the test are shown in Table XII. These quantities were calculated with the CURIE computer code [11], using a fission-product generation time of 4 msec and a total energy release of 50 megawatt seconds. A more refined estimate now indicates that the energy released during the test was on the order of 45 ± 4 megawatt seconds. In addition, the core had a prior power calibration history of 13.1 megawatt seconds [1]. (A word of caution should be noted at this point. The CURIE Code calculations rely on fission yield input data, and it appears that the direct yield of many isotopes has not been accurately measured. For instance, the direct yield of the important iodine isotope, I-131, used in the CURIE code, is 0.36 percent while other references indicate that it may be zero. This means that the code calculated quantities are not necessarily accurate.)

TABLE XII

CURIE CODE DATA FOR IODINE

Conditions:	
Generation Time	4 msec
Energy Release	50 MW-sec
Decay Time	0 sec

Isotope	$T_{\frac{1}{2}}$	Curies Available
I-129	10^7 yr	1.0×10^{-17}
I-130	---	---
I-131	8.05 day	0.16
I-132	2.3 hr	1.4×10^{-7}
I-133	20.8 hr	3.4×10^{-6}
I-134	52.5 min	77
I-135	6.7 hr	47
I-136	86 sec	1.1×10^{4}
I-137	24.4 sec	6.1×10^{4}
I-138	6.3 sec	1.6×10^{5}
I-139	2 sec	2.7×10^{5}

1.2 Iodine Released to the Cloud

Although much of the grid instrumentation was orientated towards highly sensitive detection of airborne radioactive iodine, iodine was not detected in the radioactive cloud. Several days following the test, trace quantities of iodine were detected, evolving from the environmental tank and from the vent

of the underground waste tank into which the environmental tank had been drained. Since the samplers detecting these trace levels of iodine were the same as those used on the grid (one-inch-deep beds of activated charcoal), it is concluded that trace quantities of iodine in the cloud also would have been detected.

The minimum concentration of iodine detectable by the sampling and counting system under test conditions was 8.7×10^{-9} μc/cc. This assumes 100 percent collection efficiency for the charcoal bed, a cloud sampling time of 10 seconds, and a sampling rate of 20 cfm. Using the upper limit cloud volume calculated earlier (1.45×10^{6}), this concentration yields an upper limit of 3.6×10^{-4} curies of iodine that could have been released without detection. The results of the field measurements and the sensitivity calculations, therefore, indicate that the iodine release from the destructive excursion, if any, was insignificant.

1.3 Iodine Released to the Water

Radiochemical analysis of the environmental tank water, two days following the test, showed surprisingly little iodine. The two-day delay interval reduced the amount of direct yield iodine by radioactive decay; however, if large amounts of iodine had been released, it would have been readily detectable. On the date of analysis, the environmental tank water (≈9500 gal) contained 3.15×10^{-5} μc/ml or a total of 1.2×10^{-3} curies of I-131, compared to the total available quantity of 0.92 curie calculated by the CURIE code.

Similarly, the iodine-133 data show a small amount (4.4×10^{-3} curies) of I-133 in the water, compared to the calculated quantity of 4.3 curies.

The evidence from these two isotopes of iodine indicates that the release of iodine into the water was quite low. The fraction of each would not be expected to be the same because of the difference in their direct yields, half-lives, and half-lives of their respective tellurium parents.

1.4 Iodine Retained in the Fuel

Radiochemical analysis of the twelve samples of fuel taken from fuel pin Numbers 65, 151, and 153 (Table IV) showed an average concentration of 17 μc of I-131 per gram of fuel at this time. The average value gives a total of 0.87 curie of I-131 remaining in the fuel compared with the CURIE code calculated quantity of 1.0 curie. Thus, it appears that roughly 87 percent of the I-131 was retained in the fuel. While this average value does not take into account the variation of neutron flux from sample to sample and the degree of fragmentation of fuel pins, it does serve to show that the major portion of the I-131 remained in the fuel. It can be speculated that other isotopes of iodine behaved in a similar manner.

1.5 Iodine Plate-Out

An additional location for the deposition of iodine was the surface area of the environmental tank and pipings leading from the environmental tank to the liquid waste tanks into which the environmental water was emptied. It is well known that the tellurium precursor of iodine readily plates out on vessel surfaces from an aqueous solution. This, along with the fact that iodine was detected evolving from the environmental tank following its draining, indicates that a portion of the iodine inventory was held on these surfaces. Since no specific sampling for iodine plate-out was performed quantitatively, all that

can be said is that an undetermined portion of the iodine inventory was deposited on various surfaces in the system.

1.6 Iodine Balance Summary

Although a complete accounting of the total iodine inventory was not realized, the lack of iodine in the cloud and the low concentration in the environmental tank water indicates that the majority of the iodine remained in the fuel. The radiochemical analysis of the fuel, at a somewhat later date, confirms this conclusion, indicating an iodine retention on the order of 90 percent, with the balance being plated-out on tank piping surfaces.

2. FRACTION OF NOBLE GAS RELEASE

It is not possible to perform a calculation on the quantity of radioactive gases released from a full scale reactor destructive test without necessarily making a number of assumptions. It is, however, possible, in most cases, to select a set of assumptions that can reasonably be expected to give an upper limit to the quantity released, and this mode of approach has been used in the following section. Four independent lines of approach have been used to determine the fraction of noble gases released during the destructive test.

2.1 Diffusion Calculations Using Kr-91, Kr-92, and Xe-139 Decay Chains

An estimate of the fraction of noble fission gases released to the atmosphere was made using the quantities of noble gas daughter activity collected by high-volume air samplers and an instantaneous release model. Since the high-volume air samplers did not collect the parent noble gases, correction factors for unsampled parent gases as a function of distance from the reactor were developed and applied to the measured daughter activities. After making these corrections, isopleths of the Sr-91 activity were drawn in the x-y plane at ground level (Figure 24) to facilitate the estimation of the lateral plume spread

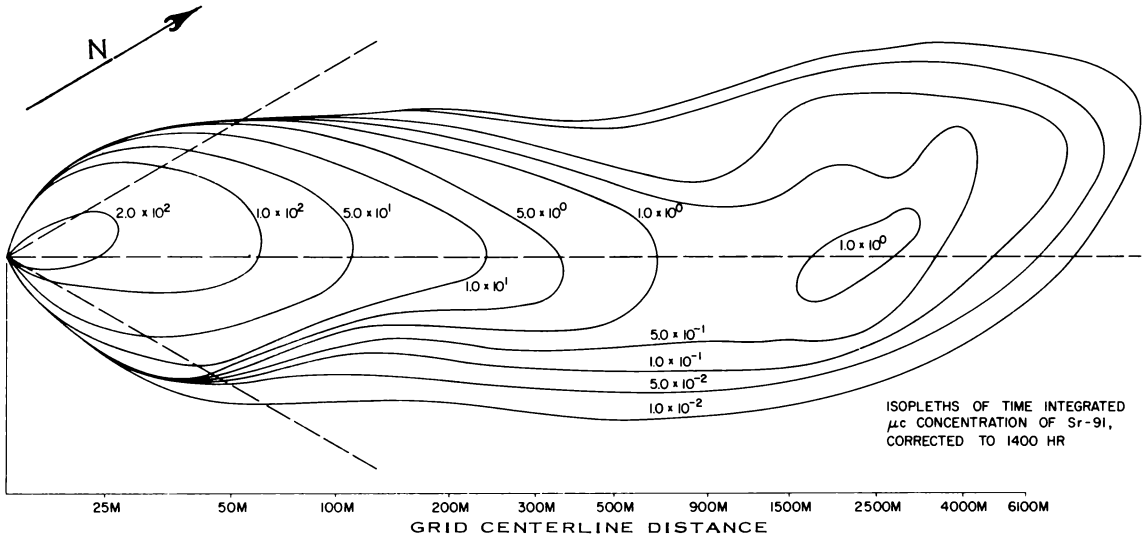

Fig. 24 Isopleths of values of μcurie-sec/m^3 for Sr-91.

and cloud centerline quantities at each sampling arc. Using these values and assuming generalized Gaussian diffusion, the analytical technique discussed in detail in Appendix A determined a release fraction of four percent for Kr-91, three percent for Kr-92, and three percent for Xe-139. One can assume comparable release fractions for other noble gases. However, the fission yields and decay modes of these other noble gases were such that their daughters were not detected by gamma spectroscopy of the air sampler filters.

Because of the uncertainties in many of the measurements and because of the series of estimates applied to the problem, it is felt that the upper limit of noble gas release determined by this method is four percent.

The summation of noble gases formed directly by the excursion was calculated by the CURIE code to be 8×10^5 curies, about 10 percent of the total fission-product inventory. One percent of the noble gases corresponds to a release of 8000 curies.

2.2 Cloud Volume Calculation -- Xe-138 Decay Chain

The noble fission gas activity from Xe-138, detected by the fission gas balloon detectors, provides another method for estimating the fraction of the noble gases released from the reactor.

The concentration of Xe-138 in the cloud, as it passed the fission gas detector at position A-3 on the 25-meter arc, was calculated as follows. At the time the balloon was deflated, there was 0.185 μc of cesium-138 collected on the balloon and exhaust filter. This corresponds to the collection of 1.4 μc of Xe-138 in the balloon during the cloud passage time. (The xenon was allowed to decay for 1.47 hr before the balloon was deflated.) Since the sampling rate of the detector was 830 cc/sec and the cloud required about 10 seconds to pass, the 1.4 μc of Xe-138 corresponds to a cloud concentration of 1.7×10^{-4} μc/cc.

From the air sampler data (Table II), it is apparent that the cloud center passed closer to station A-4 than station A-3 where the balloon detector was located and that the noble gas concentration at A-4 was nearly double that at A-3. Using this concentration factor of 2, the Xe-138 cloud concentration becomes 3.4×10^{-4} μc/cc. This concentration, coupled with the rectangular cloud volume presented earlier (4.13×10^4 m^3), yields a total release of 13.8 curies of Xe-138 or roughly 2 percent of the 630 curies produced in the excursion.

In actuality, the cloud volume was probably considerably less than the calculated rectangular shape because the dimensions used to calculate its volume were selected to provide an upper limit. Also, the overall average concentration in the cloud was probably less than the 3.4×10^{-4} μc/cc measured at ground level.

2.3 Fuel Analysis Xe-137 Chain

An indirect approach to the measurement of the release of the noble gases can be made by analyzing the reactor fuel for the quantity of the daughter activity remaining in the fuel. This approach was used on the Xe-137 decay chain by comparing the amount of Cs-137 remaining in the fuel to the amount ideally available from the total chain yield of Cs-137 for the integrated energy release from the fuel. The difference between the calculated value of the

available Cs-137 and the measured value gives the number of parent atoms (I-137 and Xe-137) that were released. By combining the fuel analysis (Table IV) with a normalized flux distribution over the core, this comparison technique indicates that an upper limit on the release fraction of the xenon-137 chain was less than 5 percent.

2.4 Kr-85 Fuel Analysis

Although the opportunities for noble gases to escape from the fuel subsequent to the test up to and during the radiochemical analysis are considerably greater than for other fission products, a direct measurement of the quantity of noble gases remaining in the fuel can be made on Kr-85 because of its 10.4 year half-life. One sample of fuel from fuel pin E-147 was analyzed and showed 3.9×10^{-3} μc of Kr-85 per gram of fuel. This value, normalized over the core, indicates that 2×10^{-4} curies of Kr-85 remained in the fuel, or nearly 80 percent of the CURIE code quantity. It is felt that this quantity is less than the percent retained during the test because of the greater opportunity for the gas to diffuse from the fuel subsequent to the destructive excursion. The results do, however, indicate that the majority of the Kr-85 remained in the fuel.

2.5 Summary of Noble Fission-Gas Release

Four independent methods were used to calculate the fraction of noble fission gases released during the power burst. Two of these depended upon actual measurement of the cloud and two on analysis of the fission products remaining in the fuel. All indicate a low percentage release.

It is felt that the diffusional calculations using the Kr-91 chain represent the most accurate determination because of the considerably larger number of measurements used to establish the model. On the basis of the assumption required to establish the diffusion model and in view of the other measurements, it appears that the percentage release of the noble fission gases should be considered to be on the order of three percent.

3. DIRECT RADIATION ANALYSES

Because little experimental information exists concerning the radiological hazards of direct radiation from this type of nuclear accident and because this particular test was initiated with the reactor already submerged in water, a theoretical analysis of the excursion has been performed. The objectives of this analysis were to confirm the accuracy of calculation techniques by comparing calculated doses to those actually measured and to predict the maximum direct radiation hazard that could occur from the water immersion of a SNAP 2/10A reactor.

3.1 Comparison of Doses

In general, the measured radiation doses included the total integrated dose from both the prompt gamma radiation and the delayed radiation from the decay of residual fission products. Since the reactor was covered with nearly four feet of water at the time of the excursion, the contribution of the prompt gammas to the measured dose was small. After the power burst, the water was drained from the tank, and the unshielded decay gammas were measured.

The points selected for comparing measured and calculated radiation doses were chosen at locations involving the simplest shielding geometry. The source geometry selected for the analytical models is as follows: a point source geometry was used for all power burst (prompt) dose calculations. For residual fission-product decay between one and ten seconds following the excursion, a cylindrical source over the entire volume of water remaining in the environmental tank (approximately eight feet deep) was used.

After ten seconds, it was assumed that all fission products were evenly spread across the floor of the tank, and a disc source geometry with the plane at the bottom of the tank was used. For points beyond ten feet to the side of the tank (in the same plane as the tank bottom), the disc source was replaced by a line source containing an equivalent amount of fission products.

The general method for determining decay radiation doses was to calculate and plot the dose rate as a function of time after the test and integrate over the appropriate period of exposure. A comparison of calculated doses to measured doses is shown in Table XIII.

TABLE XIII

CALCULATED VERSUS MEASURED RADIATION DOSES

Location	Approximate Distance From Reactor (ft)	Approximate Time of Exposure (hr)	Measured Dose (rem)	Calculated		
				Power Burst (rem)	Decay (rem)	Total (rem)
Top of Tank	8.3	24	38 (avg)	0.47	44	44.5
SW Corner of Dolly	19	24	3.3	7.7×10^{-4}	1.7	1.7
10-Meter Arc (West of Dolly)	33	3	0.35	3.6×10^{-4}	0.61	0.61
70 Feet up on Tower	90	5	0.67	6.0×10^{-2}	0.74	0.80
Detector in Reactor Tank	4	--	128	118	--	118
Clothesline above Reactor	12	3	150	6.7	162	169

The measured dose (38 rem average) at the top of the tank was detected by film dosimeters which were located several inches beyond the edge of the tank. The dosimeters were shielded from the tank floor by a portion of the concrete wall. In calculating the maximum dose of 44 rem at this location for 24 hours exposure, it was assumed that the average thickness of concrete shielding was 10 inches.

The calculated dose at the corner of the dolly is lower than the measured dose because of the assumed line source geometry (across the center of the tank) which was 19 feet from the dose point.

A comparison of calculated doses to measured film-badge doses versus height on the radiological tower, is shown in Figure 25. A point source on the the floor of the tank was assumed, and the dose for 5 hours exposure at a point 70 feet above the tank was calculated to be 6.4 rem. This was corrected for various heights on the tower by reduction due to: (a) the increased distance using the inverse square law and (b) consideration of the portion of the floor area of the reactor tank directly in "sight" of each tower height.

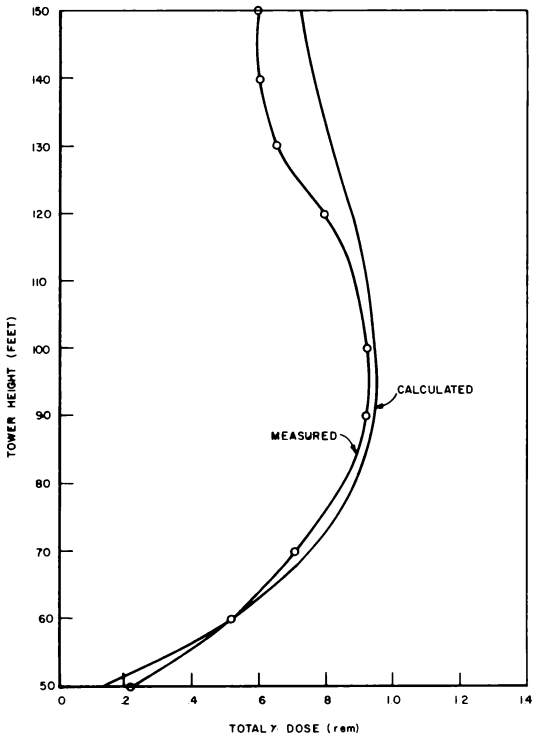

Fig. 25 Gamma dose data from radiological tower locations -- measured versus calculated.

The measured doses at tower heights above 40 feet, indicated in Figure 25, have been corrected to consider direct radiation only. It is assumed that doses on the tower below 40 feet were due only to the cloud because of the shielding of direct radiation by the reactor environmental tank, the test cell furnace housing, and various other equipment. The dose at each position above 40 feet was reduced by subtracting an effective cloud dose. This effective cloud dose was determined for each position by assuming the inverse square low-source reduction for each distance from an assumed height of 30 feet.

The power burst direct radiation was measured by means of a fast-response gamma detector located in the environmental tank approximately 4 feet away from the reactor. By integrating the area under the dose rate curve, the total burst dose for the fission and prompt gammas was obtained to be 128 rem. The calculated dose at this position was made by using a modified point source geometry, taking into consideration the self-attenuation of the core material. In addition to the fission gammas, the gammas from the neutron-water reaction and neutron-aluminum reaction were taken into consideration. The total burst dose was calculated to be 118 rem.

The highest measured dose in direct line of sight above the reactor on the clothesline was 150 rem. The calculated dose at this position was calculated using a self-attenuated point source geometry and both contributions from prompt and decay gamma radiation. The prompt radiation consisted of fission gammas and gammas produced by the neutron-water reactions. The gamma decay dose was calculated using a disc source of the floor of the tank which was shielded by the receding water remaining in the tank. The total calculated gamma dose for three hours after the test was 169 rem.

In addition to the calculated integrated doses, calculations were made to determine the gamma dose rate at the inner edge of the tank, where there was no concrete shielding involved, in order to compare with portable instrument measurements taken at this point starting about 24 hours after the test. A comparison of the measured dose rates to the calculated dose rate as a function of time is shown in Figure 26.

The equations used and the assumptions made to obtain the foregoing calculational results are given in Appendix B. It should be noted that there exist three areas of uncertainty which possibly limit the accuracy of the analytical results:

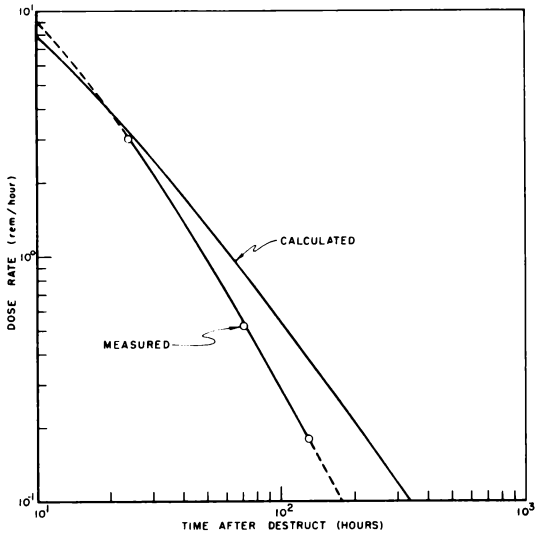

Fig. 26 Gamma dose data from locations at inner edge of environmental tank -- measured versus calculated.

(1) Analysis of the test package geometry with the complex surrounding of the tank and various equipment

(2) The exact value of the total energy release

(3) The gamma energy decay spectrum for short decay times following an instantaneous release.

The third item is due to the limit of available data concerning the activity of short-lived fission products. The spectrum used for this analysis was taken from Knabe and Putnam (Reference B-4). Their results are based on experimental data obtained at the Oak Ridge National Laboratory.

It is believed that the analytical results agree sufficiently with experimental data to justify the use of similar techniques in predicting the maximum radiological hazards due to direct radiation from a water immersion accident.

4. MAXIMUM DIRECT RADIATION HAZARD

In order to determine the maximum direct radiation hazards that could result from a SNAP 2/10A water immersion accident, consideration has been given to the case of the reactor falling into a body of water just deep enough to cover the core, thus causing the destructive excursion, but shallow enough to assume no water shielding of the radiation produced. Using the point source geometry and considering no shielding, calculations have been made to determine the total integrated dose versus distance from the reactor for an exposure period of 24 hours. Since no shielding due to water is considered, the dose from fission neutrons must be included with the dose from gamma radiation. The removal of neutrons due to oxygen in air was considered, but no self-attenuation by the reactor or shielding of gammas was included. The results are shown in Figure 27.

The primary difference in radiological hazards between this hypothetical accident and the SNAPTRAN 2/10A-3 destructive test is the difference in the initial dose from the power burst. It was shown in the foregoing analysis that the experimental power burst dose was relatively small compared to the dose from fission-product decay, due to shielding by the water in the tank. However, in the simulated maximum accident, where no water shielding is considered, the power burst dose also is significant.

If a person were to stand at a distance of 200 feet from the point of the reactor destruction, he would receive a maximum neutron dose of 65 rem

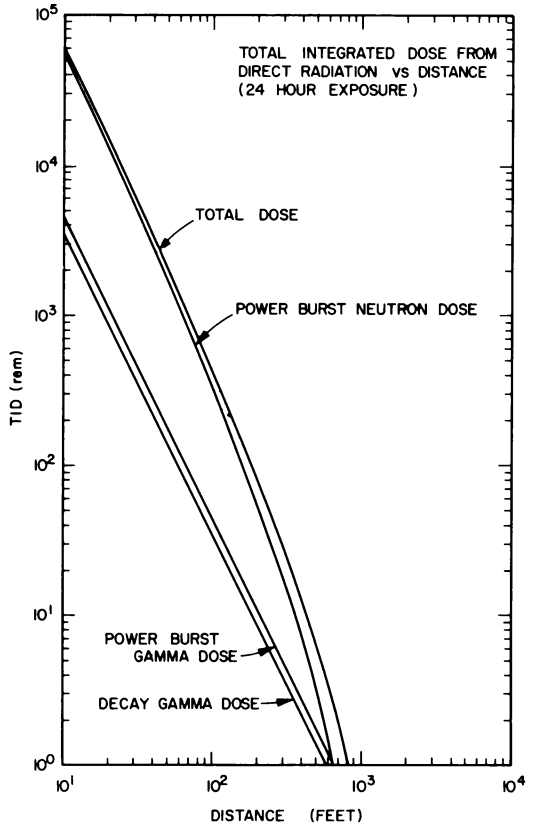

Fig. 27 Total integrated dose from direct radiation with no shielding considered.

and a gamma dose of 12 rem from the power burst and 9 rem from the decay of fission products, or a total of 87 rem for 24 hours exposure.

The data presented in Figure 27 represent a conservative approach for two reasons:

(1) In a real accident of this type, the power burst dose from fission neutrons would be much less, due to self-attenuation from the core material and shielding from the water necessary to cause the excursion.

(2) The fission products would be spread over and through a large volume of water, thus greatly reducing the intensity of the source decay radiation from that assumed in the calculational point source model.

Therefore, it is apparent that the SNAP 2/10A reactor water-immersion accident does not present a serious potential hazard to the public from direct radiation.

VII. CONCLUSIONS

The hazards involving the release of toxic and radiological material to the environment in conjunction with the destruction of a SNAP 2/10A reactor were considerably less than anticipated. The general conclusions which can be drawn from the SNAPTRAN 2/10A-3 destructive test are:

(1) No beryllium was released with the radioactive cloud.

(2) More than 99 percent of the fission products were retained in the environmental water and reactor fuel remains.

(3) Halogens, released from the fuel, were retained by the environmental tank water, with the result that no detectable iodine was released to the radioactive cloud.

(4) The radioactive cloud contained only noble fission gases and their daughters. Calculations indicate that the noble gas release fraction was less than 4 percent of the total noble gas inventory.

(5) The size of the particles released with the cloud was below the detection range of the instruments.

(6) Direct radiation hazards from the test were low. The average beta-gamma radiation dose recorded by film dosimeter, exposed for 24 hours on the top of the environmental tank, was 38 rem. The neutrons from the excursion gave a total neutron dose of 0.7 rad ten feet from the reactor. Even with the close confinement of dispersed fuel in the environmental tank, with no water shielding, the radiation levels were low, 500 mrem/hr at the top edge of the environmental tank two days after the test.

(7) There was little dispersion of radioactive debris in the vicinity of the test area. Contamination levels approached background levels three days after the test.

(8) Based on the available data, the most dependable method for determining the fission-product release from the reactor was the diffusion-type calculations based on the spread and dispersion of the radioactive cloud.

The experience gained from this test indicates that (a) better definition of the cloud trajectory and diffusion could be obtained with more closely spaced sampling stations on the monitoring arcs; (b) measurements of the cloud diffusion in the vertical direction were needed for the source term calculations; (c) earlier radiochemical analysis of the fuel would have aided in determining the fraction of the fission product retained in the fuel; (d) film dosimeters of the NRTS type with windows and shields to provide discrimination of beta exposure from gamma exposure would have provided better information than the red-plastic-sealed type used on most of the monitoring grid; and (e) continuous pen-type recorders, connected to beta-sensitive, gamma-insensitive detectors,

would have provided better definition of the cloud dynamics by responding only when in the immediate vicinity of the cloud.

In general, it can be concluded that the destructive test was successful in clearly demonstrating that a water immersion accident of a SNAP 2/10A reactor does not present a serious radiological hazard to the public. It was also successful in demonstrating the conservatism inherent in the analytical procedure for performing safety analysis on this type of reactor, eg, actual release of less than 4 percent of noble fission gases compared with the 100 percent release normally postulated.

VIII. REFERENCES

1. W. E. Kessler et al, SNAPTRAN 2/10A-3 Destructive Test Results, IDO-17019 (to be published).

2. M. Lippmann and W. B. Harris, "Size-Selective Samplers for Estimating 'Respirable' Dust Concentrations", Health Phys., 8 (March-April 1962) pp 155-63.

3. Unico Manufacturers -- Union Industrial Equipment Corporation, Port Chester, New York.

4. Research Report No. 108, Dugway Proving Grounds.

5. Gelman Instrument Company, 600 South Wagner Road, Ann Arbor, Michigan.

6. F. V. Cipperley, Private Communication.

7. F. V. Cipperley, "Improvements in Personnel-Metering Procedures at the National Reactor Testing Station", Health Phys., 4 (December 1960) pp 173-78.

8. G. S. Hurst and R. H. Ritchie (eds), Radiation Accidents: Dosimetric Aspects of Neutron and Gamma-Ray Exposures, ORNL-2748 (Pt. A) p 24 (November 1959).

9. Annual Progess Report For Health and Safety Division, Idaho Operations Office, IDO-12037, U. S. Atomic Energy Commission, (1963) p 13. (August 1964).

10. J. K. Angell, "Use of Constant Level Balloons in Meteorology", Advances in Geophysics, 8 (1961) pp 137-219.

11. N. A. Harris, G. P. Kenfield, W. R. Lahs, and W. B. Sayer, "An Improved Method of Dose Calculation from Airborne Fission Products", Health Physics, 10, P/114 (August 1964) p 615.

APPENDIX A

ESTIMATES OF ATMOSPHERIC DIFFUSION AND NOBLE FISSION-GAS RELEASE

APPENDIX A

ESTIMATES OF ATMOSPHERIC DIFFUSION AND NOBLE FISSION-GAS RELEASE

The fraction of noble gas released to the atmosphere was estimated from the quantities of daughter isotopes collected on high-volume air sample filters after accounting for: (a) radioactive decay, (b) sampling rates, (c) filter efficiency, (d) unsampled portions of parent gas, and (e) atmospheric diffusion. The analyses accounting for each factor are described as follows:

1. RADIOACTIVE DECAY

All samples were corrected for radioactive decay to a common time, 2.28 hours following the test (1400 hours, April 1, 1964).

2. SAMPLING RATES

Variance in sampling rates was accounted for by converting all sample quantities into time-integrated air concentrations with units of microcurie-second per cubic meter of air. This conversion, which was accomplished by dividing the isotopic quantities collected on the filter by the appropriate sampling rate, eliminates the sampling rate dependence between filters.

3. FILTER EFFICIENCY

Experiments at this laboratory indicate that the filter efficiency of the spun polystyrene filters for the daughter products of the noble gases is quite high ($\approx$ 100 percent). For simplicity, the filtering efficiency of these filters has been considered to be 100 percent.

4. UNSAMPLED PORTION OF PARENT GAS

If each sampler had been capable of detecting all of the fission products in one decay chain, the integrated concentration values obtained at the sampling locations would indicate the cloud spread and dilution. However, since the samplers did not sample gases, it was necessary to develop correction factors to account for the undecayed and unsampled gaseous portion of the decay chain at points near the reactor.

The release model, upon which the correction factors were developed, was one in which only noble fission gases were released from the reactor at the instant of the destructive excursion. It was also assumed that the air samplers were 100 percent efficient for the noble gas daughters.

With this release model and the general radioactive decay series of A⟶B⟶C, where A is the parent gas, B is the daughter of A, and C is the daughter of B, the correction factors were developed as follows:

$$\text{correction factor} = \frac{C_t}{C_c}$$

where C_t is obtained directly from the CURIE code and is the total quantity of the isotope C at a time, sufficiently long, after the release during which all of A had decayed. That is to say, C_t is a measure of the quantity of C which could have been collected if the samplers had collected both the gas and the daughters. And where C_c is the theoretical quantity of the isotope C, which would be obtained by collecting only the daughters, B and C, at some sampling time before all of A had decayed. That is, only B and C are collected at the sampling time, while that portion of the chain still in the form of A is lost. The quantity C_c is theoretically determined from the following equation:

$$C_c = C_s \exp\left[-\lambda_C(t_c - t_s)\right] + \frac{\lambda_C B_s}{\lambda_C - \lambda_B}\left\{\exp\left[-\lambda_B(t_c - t_s)\right] - \exp\left[-\lambda_C(t_c - t_s)\right]\right\}$$

where B_s and C_s are both obtained directly from the CURIE code and represent the amounts of B and C available for collection at the time of sampling; λ_B and λ_C are the radioactive decay constants of B and C, respectively; and t_s is the time of sampling. Sampling times were obtained from the times of peak dose rate measured by the ion chambers located at the various arcs. And t_c is the common evaluation time for C_t and for all the measured samples from the grid. The only restriction being that t_c must be sufficiently long so that all of A has decayed; ie, t_c must be greater than ten half-lives of A. Since all grid samples were corrected to 2.28 hours following the test, this value of t_c was used for all calculations.

The correction factor multiplied by the quantity of an isotope collected on a filter corrects for the unsampled portion of a decay chain due to the gaseous form of the parent.

The three observed fission-product chains were evaluated according to their decay schemes:

Kr-91 $\xrightarrow{(10\ \text{sec})}$ Rb-91 $\xrightarrow{(72\ \text{sec})}$ Sr-91 $\xrightarrow{(9.7\ \text{hr})}$ Y-91

3.45 percent

Kr-92 $\xrightarrow{(3\ \text{sec})}$ Rb-92 $\xrightarrow{(5.3\ \text{sec})}$ Sr-92 $\xrightarrow{(2.7\ \text{hr})}$ Y-92

1.87 percent

Xe-139 (41 sec) Cs-139 (9.5 min) Ba-139 (83 min) La-139

3.6 percent .

The half-lives of each isotope are in parentheses and the direct yields are given below the noble gas isotopes. The nuclear data was taken from reference A-1, except for the Xe-139 direct yield which was taken from the theoretical work presented in reference A-2.

Figure A-1 shows C_C as a function of t_S, for the three observed chains, when t_C is 2.28 hours. Figure A-2 shows the measured quantities of C as a

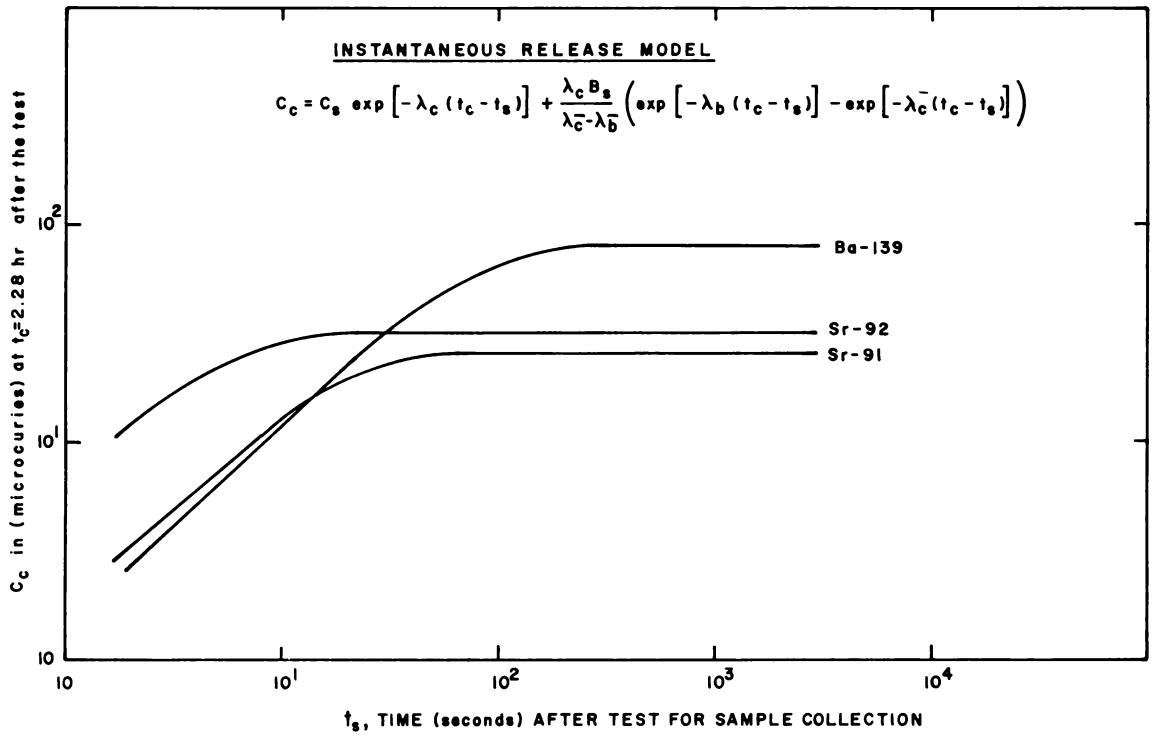

Fig. A-1 Instantaneous release model.

function of distance from the reactor. When more than one filter was available, the one with the greatest amount of radioactivity was used. The irregularities in the downward trend, with distance, are due to sampling stations off the cloud centerline and possibly due to irregularities in the terrain. The important feature of Figure A-2 is the relative amounts of the three isotopes. In comparison with the isotopic ratio predicted by the theoretical model in Figure A-1, the ratio of Sr-92 and Sr-91 does not compare favorably. In order to account for this reverse in the ratio, the release model was changed such that the noble gases were not released for approximately 3 sec following the excursion, and all of the daughters that were formed during this time remained in the environmental tank water. This assumption is borne out by the movie photographs [1] which show that the column of water above the tank existed on the order of 3 sec. This column of water could account for a delay which could cause the isotopic ratio to shift.

The modified release model suppresses the release of Kr-92 relative to the release of Kr-91 because of the shorter half-life for Kr-92. A hold up of 3 sec predicts a ratio of Sr-92 to Sr-91 in good agreement with the observed

ratio. The predicted ratio of Ba-139 to Sr-91 is larger, however, than observed, which might be explained by a preferential release of krypton over that for xenon but more probably by incorrect direct yield data used in the CURIE code.

Figure A-3 shows the measured ratios of Sr-92 to Sr-91 and Ba-139 to Sr-91 as a function of distance to the sampling arcs. It also shows the predicted ratios according to the modified model. The predicted ratios are plotted with distance instead of sampling time, t_s.

Correction factors for unfiltered noble gases were then determined from the modified release model. Corrected values of the Sr-91 integrated air concentration, measured at the time of 2.28 hours after the test, were then used to describe the meteorological diffusion over the monitoring grid.

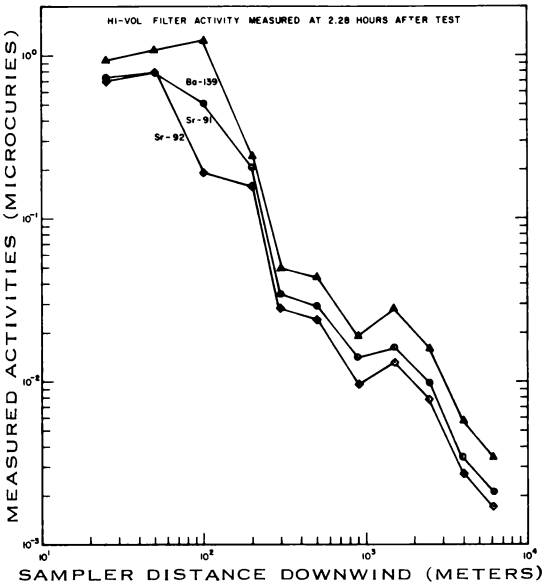

Fig. A-2 High volume activity measured at 2.28 hours after test.

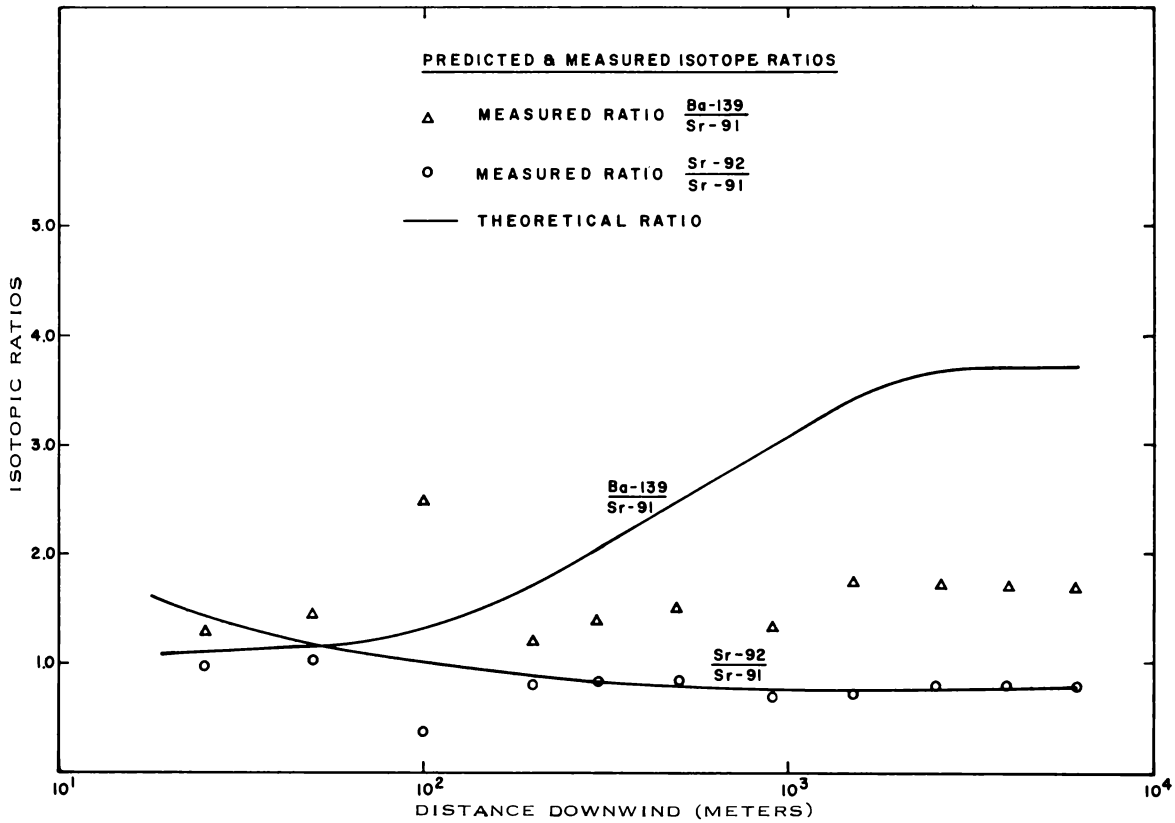

Fig. A-3 Predicted and measured isotope ratios.

Isopleths of the time integrated air concentrations at ground level were drawn, Figure 24, page 41, and were used to estimate the crosswind distributions, the lateral cloud spread, and the peak time-integrated concentration at each arc. A source term for the fission-product chain 91 was then estimated by extrapolation of the peak concentration values back to the reactor. To do this, the cloud was assumed to follow the basic meteorological diffusion equation for a ground level release:

$$\chi_p = \frac{Q}{\pi \bar{u} \sigma_y \sigma_z}$$

where

χ_p is the peak time-integrated concentration at downwind distances

Q is the source term, curies released

$\bar{u}$ is the mean wind speed, meters per second.

σ_y is the lateral cloud spread, meters

σ_z is the vertical cloud spread, meters.

Figure A-4 shows the measured σ_y values plotted as a function of distance, x. The solid line indicates the regression line, $\sigma_y = 0.20x^{0.85}$, fitted to the values. This lateral cloud spread compares very well with other NRTS measurements made by the U. S. Weather Bureau for 30-minute tracer releases under similar meteorological conditions. The information from these longer releases and the wind, horizontal turbulence measurements during the test would predict $\sigma_y = 0.18x^{0.875}$. Measurements at other sites have been summarized into an atmospheric stability classification system that predicts σ_y and σ_z values for 10-minute releases under various conditions (Reference A-3). For the test meteorological conditions, the σ_y values predicted are indicated in Figure A-4 by the dashed line. In contrast to the measured σ_y parameter, essentially no measurements of the vertical cloud spread, σ_z, were obtained. Therefore, an estimate of the σ_z parameter was necessarily used in determining the source term, Q.

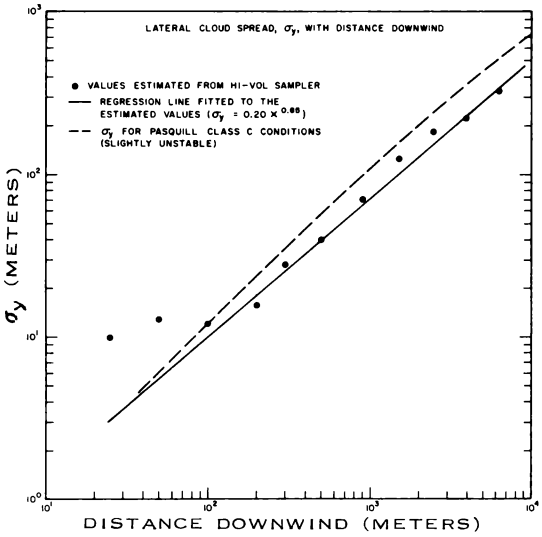

Fig. A-4 Lateral cloud spread, σ_y, with distance downwind.

Figure A-5 shows the peak time-integrated concentrations, χ_p, for each arc as estimated from the isopleth figure. Four different curves have been drawn through these points in order to bracket the actual source term. Curves one through three assume a ground level release while curve four assumes an above ground release in order to obtain a maximum source term value. Four source terms are calculated from the extrapolated ordinate intercept of each of the four curves.

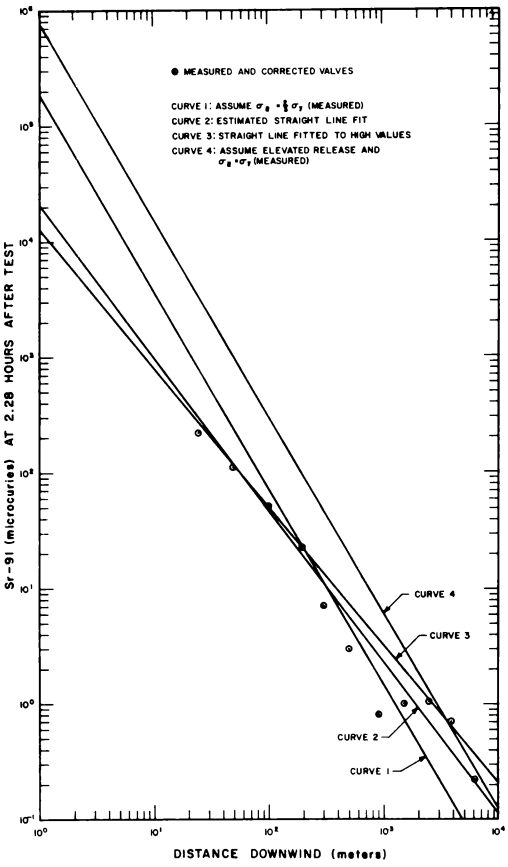

Fig. A-5 Peak time -- integrated concentrations at each sampling distance downwind.

Curve 1: Experience at the NRTS suggests that an estimate of $\sigma_z = 2/3\ \sigma_y$ is reasonable for the test meteorological conditions. This relationship can also be inferred from the vertical turbulence measurements which indicate that the vertical turbulence during the test was about two thirds of the horizontal turbulence at 60 meters above the surface. With this approximation the peak concentration (χ_p) dependence on distance is proportional to $x^{-1.7}$. A curve with this slope drawn through the measured χ_p values yields a source term of Q = 1.5×10^5 microcuries.

Curve 2: An "average" straight line drawn through the measured χ_p values shows a distance dependency of $x^{-1.32}$. This results in a source term of Q = 2.2×10^4 microcuries.

Curve 3: A straight line was drawn through the largest χ_p values. This estimate assumed that the cloud "bounced" across the grid and that the largest measured values represent the actual diffusion with distance. This estimate gives a distance dependence of $x^{1.20}$ which yields a source term of Q = 1.3×10^4 microcuries.

Curve 4: This curve is based on a set of assumptions intended to give the maximum value of Q. NRTS experience indicates that for the slightly unstable conditions observed during the test the distance dependency of σ_z will not exceed that of σ_y. Using the maximum conditions of $\sigma_z = \sigma_y$ and the measured value of $\sigma_y = 0.20\ x^{0.85}$ yields a curve with a slope of -1.7. The maximum value of Q is then obtained by drawing a curve with this slope through the highest measured values of χ_p with respect to distance. The points from the last three arcs on the grid represent the highest values of χ_p with respect to distance.

The use of the last three points is based on the hypothesis that the radioactive cloud was released at an elevation of approximately 10 meters. The cloud was then assumed to remain at a constant level above the ground out to about 1600 meters where terrain takes a sharp rise of about 10 meters. At this point it is assumed the terrain intersected the cloud trajectory and measured values of χ_p from the three remaining arcs represent true ground level diffusion. A curve with a slope of -1.7 drawn through the measured values of χ_p from the last three arcs gives an extrapolated source term of Q = $\underline{1.0 \times 10^6}$ microcuries.

The source terms calculated from the extrapolated curves are the microcurie amounts of Sr-91 at the time of 2.28 hours after the test assuming a puff release. According to the CURIE code calculations, the total Sr-91 inventory available from its krypton parent at this time was 25.6 curies. Comparing the largest or upper limit extrapolated source term with this inventory determines

a release fraction for the Kr-91 decay chain of about 4 percent. By similar comparisons, the upper limit release fraction for the Xe-139 chain was about 3.0 percent and for the Kr-92 chain about 3.0 percent.

It is expected that a more realistic upper limit of release would be obtained using the values of $\sigma_z = 2/3\ \sigma_y$ since this relationship is more nearly what would be expected under the weather conditions of the test. This would reduce the Kr-91 chain release to approximately 3 percent and the Xe-139 and Kr-92 chain to 2 percent.

II. REFERENCES

A-1. S. Katcoff, "Decay Chains and Yields from Thermal-Neutron Fission of U-235", Table 3, Nucleonics, 18 (November 1960) p 205.

A-2. R. D. Present, "On the Division of Nuclear Charge in Fission", Phys. Rev., 72 (July 1947) pp 7-15.

A-3. F. A. Gifford, Jr., "Atmospheric Dispersion Calculations Using the Generalized Gaussian Plume Model", Nucl. Safety, 2 (December 1960) pp 56-59.

APPENDIX B

~~DIFFUSION CALCULATION TECHNIQUES~~

TECHNIQUES FOR DIRECT RADIATION CALCULATION ← ERRATA

APPENDIX B

~~DIFFUSION CALCULATION TECHNIQUES~~

Techniques For Direct Radiation Calculation ← ERRATA

I. ANALYTICAL TECHNIQUES -- EQUATIONS USED

1. DIRECT RADIATION FROM POWER BURST

Calculations of gamma doses from the power burst were based on the following equation, assuming a point source geometry [B-1].

$$D_\nu \text{ (rem)} = K_e \, B \, \frac{S_o \, e^{-b_1 (t)}}{4\pi \, a^2}$$

where

D_ν = gamma dose at P_1, the point under consideration

B = gamma dose buildup factor, based on external shield

S_o = source strength, $\frac{\nu \text{'s}}{\text{sec}}$ of energy $E = 3.1 \times 10^{10} \, P \, N(E)$

P = average power of the burst

N(E) = source spectrum for prompt fission ν 's = 2.89 $\frac{\text{MeV}}{\text{fiss}}$ at 0.8 MeV, 2.26 $\frac{\text{MeV}}{\text{fiss}}$ at 2 MeV, and 2.04 $\frac{\text{MeV}}{\text{fiss}}$ at 4 MeV [B-2].

a = distance from source to dose point, cm

$b_1 = \sum_{i=1}^{n} \mu_i \, t_i$

μ_i = macroscopic cross section (linear absorption) of the ith external shield, cm^{-1}

t_i = shield thickness, cm

K_e = conversion from gamma flux to dose rate [B-1], rem/hr per $\frac{\nu}{\text{cm}^2\text{-sec}}$, a function of gamma energy

(t) = time duration of the power burst.

NOTE: The point source was assumed to be inside the cylinder with effective external shielding equivalent to the self-shielding of the cylinder plus the shielding external to the cylinder. The effect of self-shielding was determined to be a reduction in the total dose by approximately a factor of ten.

In calculating the total dose for the maximum simulated accident, the effect of self-attenuation was neglected. The neutron dose was calculated using the point source equation with attenuation due to removal by oxygen in air. The conversion from neutron flux to dose rate [B-1], rem/hr, was based on an assumed neutron energy of one MeV.

2. DIRECT RADIATION FROM FISSION-PRODUCT DECAY

Calculations of gamma dose rates from fission-product decay were based on the following equations:

2.1 Disc Source [B-1]

$$D_\gamma \left(\frac{\text{rem}}{\text{hr}}\right) = K_e \frac{B\, S_A}{2} \left[E_1 (b_1) - E_1 (b_1 \sec \theta)\right] K \left(\frac{d}{R_o}, \frac{h}{R_o}, \bar{u} R_o\right)$$

where

S_A = source strength, $\frac{\gamma\text{'s}}{\text{cm}^2\text{-sec}}$ of energy $E = 3.1 \times 10^{10}$ $P\, t_o a\, \frac{M(\infty, t_s)}{t_s} f(t)$, divided by the area of the tank floor, cm^2

Pt_o = total energy release, watt-sec

$M(\infty, t_s)$ = At^{-a} where A and a are constants for shutdown time interval under consideration [B-3]

$f(t)$ = fraction of total gamma energy for each effective energy group (0.9, 1.8 and 2.6 MeV) at shutdown time t_s for an instantaneous release [B-4]

$$E_1(b_1) = \int_{b_1}^{\infty} \frac{e^{-t}}{t}\, dt$$

$$E_1(b_1 \sec \theta) = \int_{b_1 \sec \theta}^{\infty} \frac{e^{-t}}{t}\, dt$$

θ = $\tan^{-1} \frac{R_o}{h}$

R_o = radius of tank, cm

h = height of tank, cm

$K\left(\frac{d}{R_o}, \frac{h}{R_o}, \bar{u}R_o\right)$ = correction for distance, d, from vertical axis to dose point, taken as 1 to produce maximum results.

The other quantities are as previously described.

2.2 Line Source [B-1]

$$D_\nu \left(\frac{rem}{hr}\right) = K_e \, B \, \frac{S_L}{2\pi a} \, F(\theta_1, b_1)$$

where

S_L = source strength, $\frac{\nu's}{cm\text{-}sec}$, of energy $E = 3.1 \times 10^{10}$ $Pt_o a \, \frac{M(\infty, t_s)}{t_s} \, f(t)$ divided by the diameter of the tank, cm

a = distance from center of tank to dose point

$F(\theta_1, b_1) = \int_0^{\theta_1} e^{-b_1 \sec \theta'} \, d\theta'$

$\theta_1 = \tan^{-1} \frac{R_o}{a}$.

The other quantities are as previously described.

2.3 Cylindrical Source [B-1]

$$D_\nu \left(\frac{rem}{hr}\right) = K_e \, B \, \frac{S_V \, R_o^2}{4(a + z)} \, F(\theta_2, b_2)$$

where

S_V = source density, $\frac{\nu's}{cm^3\text{-}sec}$, of energy $E = 3.1 \times 10^{10}$ $Pt_o a \, \frac{M(\infty, t_s)}{t_s} \, f(t)$, divided by the volume of water remaining in the tank immediately after the test, cm^3

z = effective self-absorption thickness of the homogeneous source, cm

a = distance from inside wall of tank to dose point, cm

$\theta_2 = \tan^{-1} \frac{h}{a + z}$

h = height of water in tank, cm

$b_2 = b_1 + \mu_s z$

μ_s = macroscopic cross section (energy absorption) of water.

The other quantities are as previously described.

The integrated gamma dose for an exposure time, t sec, was found by integrating under the curve of dose rate (rem/hr) versus time, plotted on a log-log graph, using the following equation:

$$TID(rem) = K \int_{t_1}^{t_2} t^{-\alpha}\, dt$$

where

α = slope of decay curve at time, t

t_1, t_2, = initial and final times governed by slope, α, for partial integration, sec

K = effective dose rate at 1 sec for curve with slope, α, rem/sec.

II. ASSUMPTIONS

Calculations of all direct radiation doses were based on the following assumptions:

(1) The excursion produced an energy release of 50 MW-sec [1].

(2) All fission products were contained in the tank and uniformly dispersed on the floor.

(3) Approximately 8 feet of water remained in the tank for 30 seconds after the test. It was pumped down to 2-1/2 feet during the interval from t + 30 seconds to t + 11 minutes, and it was drained completely after 4 hours.

(4) External shielding consisted only of water and 2 feet of concrete.

(5) Point source geometry for power burst calculations with an effective external shield equivalent to the self-shielding of the cylinder plus the shielding external to the cylinder.

(6) Disc source geometry (on floor of tank) for decay calculations at top of tank after 10 seconds.

(7) Line source geometry for decay calculations beyond 10 feet from the tank after 10 seconds.

(8) Homogeneous cylindrical source geometry for decay calculations at 1 second after test.

(9) Three effective gamma energies for power burst calculations: 0.8, 2.0, and 4.0 MeV [B-1].

(10) Three effective gamma energies for decay calculations: 0.9, 1.8, and 2.6 MeV [B-3].

III. REFERENCES

B-1. T. Rockwell, III (ed.), Reactor Shielding Design Manual, TID-7004 (March 1956).

B-2. Niel Cook, "Bettis Reactor Engineering School Radiation Shielding Course Notes", June 1959, Rev. (August 1961).

B-3. K. Shure, Fission Product Decay Energy, WAPD-BT-24 (December 1961) pp 1-17.

B-4. W. E. Knabe and G. E. Putnam, The Activity of the Fission Products of U-235 APEX-448 (October 1958).

ERRATA FOR IDO-17038

RADIOLOGICAL ASPECTS OF
SNAPTRAN 2/10A-3 DESTRUCTIVE TEST

Page 2, Figure 1 - 8.907" Dia. should read 8.939" Dia.

1.212" Dia. should read 1.25" Dia.

Pages 61 and 63 - The title heading for Appendix B should read:

"TECHNIQUES FOR DIRECT RADIATION CALCULATION"

M. Z. 4/16/66

PHILLIPS
PETROLEUM
COMPANY

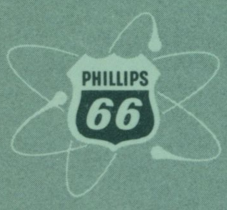

ATOMIC ENERGY DIVISION